American Journal of Science

ATOMISTIC TO MESO-SCALE MODELING OF MINERAL DISSOLUTION: METHODS, CHALLENGES AND PROSPECTS

INNA KURGANSKAYA*,† and RICARDA D. ROHLFS*

ABSTRACT. Dissolution and growth of minerals constitute a special interdisciplinary field covering a large variety of modern ecological and geochemical problems, for example, radioactive and toxic waste sequestration, weathering and biomineralization. The processes of mineral dissolution and growth are inherently complex. Formulation of a consistent theory applicable to arbitrary environmental conditions is a big goal for the geochemical community. This task cannot be fulfilled without a rigorous systematic methodological approach to create multi-scale models. We review current modeling approaches from atomistic to meso-scale as well as state-of-the-art approaches to connect these scales. Atomistic models provide us with molecular reaction rates and help us to explain mechanisms of bond dissociation, formation of transition state and adsorption complexes. Kinetic Monte Carlo (KMC) models incorporate an ensemble of different elementary reactions taking place at mineral surfaces. These stochastic models provide us with reaction sequences and corresponding surface topographies, as well as the geometry of reactive surface features. Experimental measurements provide important material for model verification. Environmental controls of the reaction process are incorporated into KMC models by using complementary Grand Canonical Monte Carlo (GCMC) simulations that provide statistics on charged sites and adsorbed ions. Reactive Canonical Monte Carlo constitutes an alternative approach to study mineral-fluid systems at chemical equilibrium. Analytical models of dissolution and growth based on atomic step velocities as functions on elementary rates and environmental conditions have been actively developed for decades. A novel, fast approach based on computational geometry, using Voronoi surface partitioning with non-Euclidean distance function, recently appeared. This approach allows us to simulate systems larger than what can be handled with atomistic methods and enables the possibility to upscale all-atomic meso-scale models to pore and continuum scales. The aim of this manuscript is to provide a road map of the existing vibrant field of atomistic-to-meso-scale models and computer simulations. We supplement the text with important equations quantitatively relating physical parameters involved in models at different scales. The discussion of existing methodological gaps and lack of parameters necessary for the construction of multi-scale models is provided.

Key words: mineral dissolution, stochastic modeling, Monte Carlo, Voronoi model, multi-scale, mineral-water interface

INTRODUCTION

Mineral dissolution and growth kinetics nowadays can be considered as a special discipline incorporating broad knowledge from many fundamental disciplines: mineralogy, geochemistry, physical chemistry, chemistry of surfaces and colloids, hydrogeology, solid state physics and chemical physics. The essential core of the discipline is the interaction of the solid material with the liquid phase commonly represented by water with any dissolved components. The process can be considered at a wide range of

* University of Bremen, FB5 and MARUM, Klagenfurter Str. 4, 28359 Bremen, Germany
† Corresponding author: inna.kurganskaya@uni-bremen.de

spatial and temporal scales, from electronic density structure at subatomic scale to meters and kilometers of metasomatically replaced mineral phases, from femtoseconds corresponding to fractions of atomic vibration frequencies to thousands and millions of years corresponding to geological time scales. Complexity of the dissolution process at any scale stems from a great number of possible degrees of freedom, for example chemical composition and crystal structure, order-disorder of cations in crystalline lattice (Zhang and Lüttge, 2007; Zhang and Lüttge, 2008; Yang and others, 2014), variations in grain size (Briese and others, 2017) and crystal defect distributions (Fischer and others, 2014; Fischer and others, 2018). Chemical composition of the interacting fluid coupled with material transport phenomena is another source of variance (Colombani, 2016), introducing influence of the saturation state, pH, ionic strength and other chemical dependencies (Brantley and others, 2008). Long-term attempts to calculate dissolution rate constant as a ubiquitous stable environment-independent parameter showed that its variance may span up to three orders of magnitude (Lüttge and others, 2013). Therefore, apart from external environmental parameter variance, for example saturation state, intrinsic variation pertaining to the solid material itself is an essential part of the dissolution process (Lüttge and others, 2013). Variance in dissolution rates at fixed thermodynamic conditions for the same material had been shown in experiments (Arvidson and others, 2003; Fischer and others, 2012). These results inevitably exhibit that common empirical assumption about simple zero, first or second order kinetics, theoretically justified and employed for molecular reactions in the gas phase, in many cases cannot be applied for solid materials. Instead, in physical terms, the dissolution process can be represented as a complex reaction network incorporating different parameters and factors. The mechanistic nature of the dissolution process is specific for each spatial and temporal scale. Any quantitative predictions of the kinetic behavior of solid materials for natural and man-made systems must consistently incorporate the information about the process obtained at different scales. This challenging task requires good understanding of dissolution mechanisms and reaction network dynamics across the scales, as well as the connection of the processes and kinetically relevant factors between the scales. At the moment, these scale-connecting interfaces do not exist as well-developed and widely accepted methodological approaches. In the modern computer era numerical approaches provide a great opportunity to construct and test mechanistic models of the dissolution process at different scales. In this paper we provide a brief overview of commonly used modeling techniques covering atomistic to meso scales and discuss the ways to connect them. The number of studies in this area is tremendous and it can be hard to cover all the aspects. Due to this reason, we focus on the methods and processes that are important for understanding qualitative and quantitative relationships between the molecular scale reactions and microscopic scale processes.

ATOMISTIC SCALE

Quantum Mechanics

Quantum Mechanics (QM) is a cornerstone theoretical tool of modern chemistry. The major idea behind the QM methods in chemistry is to describe electronic structure of atoms, molecules and chemical bonds. Chemical reactions at the molecular scale are well-described as changes in the electronic density at the processes of bond breaking and forming. The energy of an atomic-electronic system can be calculated from the Schrödinger equation that in the time-independent form has the following generic expression(Ratner and Schatz, 2000):
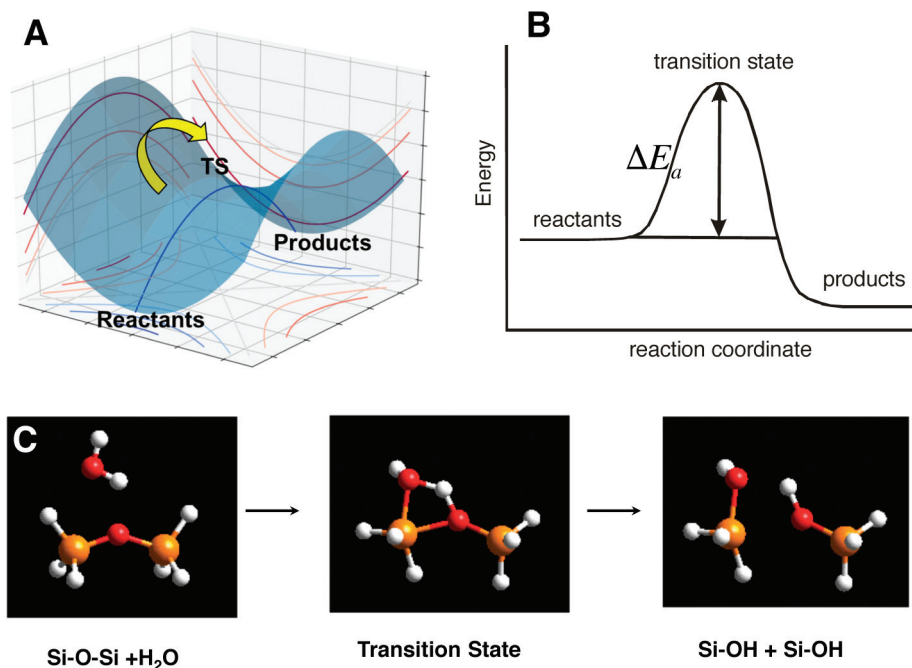
$$\hat{H}\psi = E\psi, \tag{1}$$

Fig. 1. Dissolution reaction mechanism at the atomistic level according to the Transition State Theory. (A) Potential Energy Surface (PES) model around a transition state [the image is produced by using Matplotlib graphical package (Hunter, 2007)]. (B) Activation energy barrier along a reaction path. (C) Si-O-Si bond hydrolysis by a water molecule via a transition state [generated using GaussView program (Dennington and others, 2009)].

where ψ is the time-independent wavefunction, $\hat{H}$ is the Hamiltonian operator defined for a system of interest. It is possible to move positions of nuclei in space and map out the system's potential energy as a function of atomic positions or other "degrees of freedom". In this case, a potential energy surface (PES) can be constructed. The PES is crucial for determination of the reaction mechanisms and calculations of reaction rates according to the Transition State Theory (Eyring, 1935). Reactants and products, as stable atomic configurations, can be located at the potential wells – local minima of the PES. Two neighboring potential wells are separated by a "ridge" that needs to be crossed, the most probable pathway comes through a minimum of that "ridge" defined as a saddle, or transition state point (fig. 1A). The reaction rate then is a function of the minimal energetic barrier separating reactants and products (fig. 1B). The rate and the energy barrier are related via a simple equation given by Eyring (Eyring, 1935):

$$k = \kappa \, \frac{k_B T}{h} \frac{Q_\ddagger}{Q_A Q_B} e^{-\frac{\Delta E}{RT}} \qquad (2)$$

where k is the reaction rate, κ is the transmission coefficient taking into account crossing and recrossing back the barrier, k_B is the Boltzmann constant, T is the temperature, h is the Planck's constant, R is the universal gas constant, ΔE is the energy of the activated complex, $Q_\ddagger$, Q_A and Q_B are the partition functions for the activated complex and the reactants, A and B. Typically, in the *ab initio* studies the transition state is identified, and its energy and partition function are calculated.

QM theoretical apparatus may then provide an inevitable insight into mechanisms of mineral surface reactions and supply values of molecular reaction rates. Dissolution reaction at the molecular scale can be described as a bond breaking process where coordination of a surface group by its lattice neighbors changes to coordination by water molecules (fig. 1C). The activation barrier for such a reaction depends on chemical and geometric factors. The difference in the activation energies of bond breaking for Si-O-Si and Si-O-Al dimers (Xiao and Lasaga, 1996) can be used to explain the difference in dissolution rates for quartz and feldspars (Brantley and others, 2008). The effects of pH onto bond breaking energies can be captured by protonating bridging O and deprotonating dangling OH^- groups (Morrow and others, 2009). Size of the simulation cluster may play a pivotal role in defining bond breaking activation energy, major effect comes from the number of neighbors for bond-forming sites. This "lattice resistance" effect was demonstrated for silica (cristobalite) clusters. The activation energy for Si-O-Si bond was shown to be controlled by the bond topology denoted as Qi-Qj, where *i* and *j* are numbers of bonds at Si sites (Pelmenschikov and others, 2000). The effect of cluster size and topology onto site reactivity and acidity was shown to have importance for reactive properties of metal oxides (Casey and Swaddle, 2003). The structure of the water layers adsorbed at particular mineral faces significantly influences their energetic stability (Murashov, 2005; Yang and Wang, 2006), potential reactivity and dissolution rates of these faces (Nangia and others, 2007). Presence of ions may substantially alter interfacial water layer structure resulting in change of reaction mechanisms, activation energies and rates (Kubicki and others, 2012). In general, the organization of water molecules at mineral interfaces depends on different factors, for example, mineral chemistry, exposed face, presence of defects, as well as the presence of adsorbed ions and other interface components. These details define local site acidity, vibrational properties of sites and interfacial water molecules, and other molecular details influencing site reactivity (Gaigeot and Sulpizi, 2016).

The major limitation of the *ab initio* methods is the system size. The construction of the PES surface and search for transition state for complex solid-fluid systems by using pure *ab initio* methods is problematic due to the rough structure and dimensionality of PES (Gross, 2000). Vast majority of the endeavors in the modern studies of reaction mechanisms and rates for solid surface reactions are concentrated in the Molecular Dynamics field allowing to model bigger systems where the tools of the statistical mechanics can be applied.

Molecular Dynamics

Molecular Dynamics (MD) simulations have tremendous potential for the understanding of many-body system dynamics. In MD simulations, atoms are treated as classical bodies moving according to the Newtonian laws (Allen and Tildesley, 2017). The forces defining atomic motion are calculated as gradients of the potential energies U arising from the atomic interactions:

$$m_i \frac{d^2 r_i}{dt^2} = \sum_{i \neq j} f_{ij}(r_{ij}) = -\nabla_i U(r^N). \tag{3}$$

Here m_i is the particle mass, r_i is the coordinate vector, f_{ij} are interaction forces with the other particles, *U* is the potential energy as a function of the position of *N* particles (Lesar, 2013).

The energies can be calculated by using pre-developed force fields (FF), or directly using QM methods. For example, in *ab initio* Molecular Dynamics (AIMD) (Tuckerman, 2002; Kühne, 2014), the forces are calculated on-the-fly by using *ab initio*/Density Functional Theory. Most of the FF were developed for bonded systems, for example UFF, the universal force field (Rappe and others, 1992), CLAYFF (Cygan and others, 2004), the

force field for clay minerals and silicates, first force fields for carbonate minerals (Pavese and others, 1996; de Leeuw and others, 1999). Generally, these force fields are employed for studying non-reactive interactions of water with mineral interfaces. Wolthers and others (2013) used the force field developed specifically for carbonate-water interfaces (de Leeuw and Parker, 1998) to calculate frequencies of water molecules exchange at different reactive sites on a calcite surface. Their results show that interfacial water dynamics at different surface sites have drastically different kinetic behavior: water at terrace sites is two orders of magnitude less mobile than at kink sites.

Dissolution reactions require lattice bond breaking and formation, it is commonly achieved by calculating bond parameters from local coordination (Senftle and others, 2016). This methodology was applied to develop the reactive force field for carbonate mineral-water system (Raiteri and others, 2010; Gale and others, 2011; Raiteri and others, 2015). This force field was used to understand energetics of calcium and carbonate adsorption and incorporation at the step site during the process of calcite growth.

Calculation of the Gibbs free energy surface (FES) instead of PES is commonly done in MD simulations dedicated to the studies of surface reactions. In this case there is no need to calculate partition functions explicitly since their expressions for the surface reactions can be complex or not well-defined (Jansen, 2012). The elementary reaction rate in the free energy formulation is derived by Eyring, Polanyi and Evans (Evans and Polanyi, 1935; Eyring, 1935; Laidler and King, 1983) in The:

$$k = \kappa \frac{k_B T}{h} e^{-\frac{\Delta^\ddagger G}{RT}} = \kappa \frac{k_B T}{h} e^{\frac{\Delta^\ddagger S}{R}} e^{-\frac{\Delta^\ddagger H}{RT}}, \qquad (4)$$

where $\Delta^\ddagger G$, $\Delta^\ddagger S$ and $\Delta^\ddagger H$ are the Gibbs free energy, entropy and enthalpy change between the transition state and the reactants (Eyring, 1935). As it can be seen from the (eq 4), the temperature-dependent term that gives the Arrhenius activation energy E_a depends only on the enthalpy, while the entropy term is temperature independent and contributes to the Arrhenius pre-factor A in the equation:

$$k = A e^{-\frac{E_a}{RT}}. \qquad (5)$$

Therefore, in the cases of large entropic differences between reactants and the transition state, the apparent activation energy in experiments is expected to be smaller than the total energetic barrier, but the pre-factor values would be larger (Campbell and others, 2013).

The free energy landscape can be used to identify possible reaction mechanisms and locate transition states. This step is necessary to perform before starting any rate calculations. Thus, free energy surfaces FES were constructed for the dissolution reaction from gibbsite surface (Shen and others, 2018). This allowed them to identify the kink site formation mechanism as rebounding of an Al tetrahedron to the ledge as an adatom with the subsequent detachment. A similar strategy was used to investigate dissolution mechanisms from the ledge sites of goethite. Fe ion detachment was found to proceed via two different mechanisms: (1) reduction of Fe(III) to Fe(II) in the lattice with the subsequent fast release, (2) protonation and hydrolysis of a bridging bond (Klyukin and others, 2018).

As it can be found from the (eq 4), Gibbs free energy landscapes can be used to estimate reaction rates. Kerisit and Parker (2004) calculated rates for adsorption and desorption of ions at calcite-water surface from the equation:

$$k = \kappa k^{TST}, \qquad (6)$$

where κ is the transmission constant, k^{TST} is the transition state coefficient, calculated from the Gibbs free energy profiles (Kerisit and Parker, 2004; Stack and others, 2012).

Calcium ion was found to be more mobile than carbonate as reflected in the values of adsorption and desorption frequencies.

Since resolution of the simulation system must be a fraction of atomic vibration frequency (femtoseconds), the total simulation trajectories typically do not exceed a nanosecond. This time frame is too short for calculations of atomic detachment rates. In order to overcome this limitation, the metadynamics – a fast method of energy landscape exploration – is used (Laio and Parrinello, 2002). According to this method, the system is forced to effectively explore new regions of space instead of spending most of time in potential wells. This is achieved by "filling" the wells with artificial potential and "pushing out" the system from the potential well. This method, combined with the reactive flux sampling, was used to calculate rates of detachment and attachment of a barium ion from and to an atomic step (Stack and others, 2012). They used the same TST free-energy based approach as mentioned above to calculate rate constants for detachment of a barium ion from a kink site on a barite surface. This reaction was broken into distinct steps of the sequential bond breaking, formation of outer sphere complex, and desorption of this complex from the surface (figs. 2A-2E). Overall constant for each bond-breaking and detachment step was calculated according to the (eq 6) from free energy barriers (fig. 2E) and transmission coefficients. The first bond has the largest barrier to break and reforms faster than it breaks, the second bond is looser and breaks faster and does not tend to reform, while the adsorbed inner-sphere complex (one-bonded ion) tends to stay on the surface (Stack and others, 2012). A similar mechanism was found for the dissolution at a kink site of NaCl (Liu and others, 2011), where two transition states characterized by different bonding environments and one intermediate inner-sphere adsorbed state were identified (figs. 2F-2J), and the free energy maps were constructed (fig. 2K). In general, published MD studies provide two types of data for the kineticists: (1) free energy landscapes with the barrier values; (2) TST rate constants for the molecular reactions.

QM and MD methods applied to study geochemical reactions constitute a large research area that is not possible to cover in one paper. We further refer the reader to the recently published textbook (Kubicki, 2016).

<div align="center">MESO-SCALE</div>

<div align="center">*Kinetic Monte Carlo*</div>

Kinetic Monte Carlo simulation is aimed to provide temporal evolution of a reactive system defined as a set of possible reactive events. Every reaction is chosen randomly with the frequency corresponding to its probability. The exact derivation of the KMC method is provided in the early work of Gillespie (Gillespie, 1976). The method was developed as a stochastic simulator of chemical reactions in the gas phase with the aim to take into account stochastic effects inherent to reactive system of interest. The method was used to simulate growth of a Kossel crystal – the simplest model of a crystalline body with primitive cubic cell (Kossel, 1927; Stranski, 1928). The events are defined by their rates that are converted into probabilities by using a generic formula:

$$P_j = \frac{k_j}{\sum_{j=1}^{N} k_j}, \qquad (7)$$

where k_j is the rate of a jth event out of N events in total.

The method received wide recognition with regard to the studies of crystal growth as atomic deposition at surface atomic steps (Gilmer, 1976; Cherepanova, 1981; Cheng and Coller, 1987; Cheng and others, 1989) following the BCF theory of crystal growth
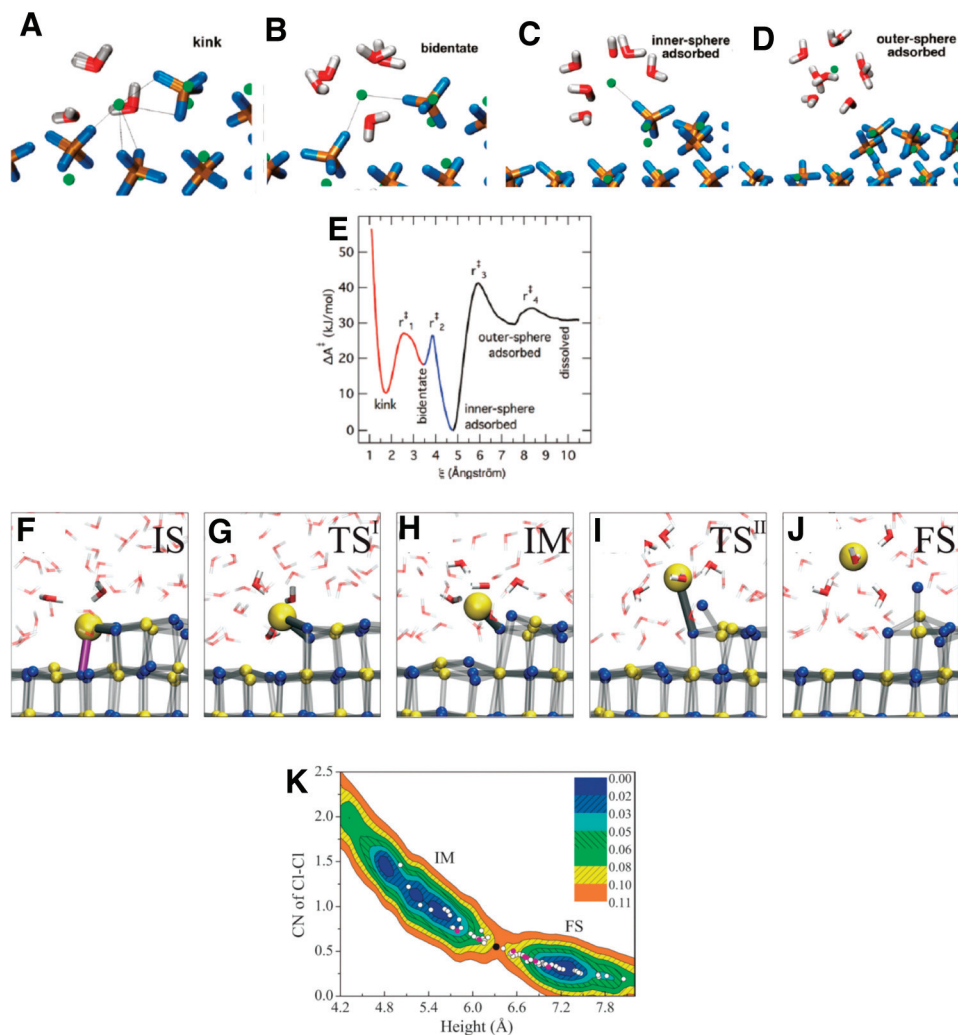
Fig. 2. Elementary steps for the dissolution process at kink sites, Molecular Dynamics simulations. (A)-(E). Dissolution of Ba^{2+} from barite kink site. (A) Hydrated ion at the kink site. (B) Bidentant two-coordinated ion. (C) Inner-sphere adsorbed complex (one-bonded). (D) Outer-sphere adsorbed fully hydrated ion (zero-bonded). (E) Free energy profile. Reprinted (adapted) with permission from (Stack and others, 2012). Copyright (2012) American Chemical Society. F-K. Dissolution of Cl^- from halite kink site. (F) Initial state. (G) Transition State 1. (H) Intermediate state. (I) Transition State 2. (J) Final state. (K) Free energy map in coordinates of collective variables (see reference) showing transition from the intermediate to final state via Transition State 2. Reproduced from (Liu and others, 2011) with permission from the Royal Society of Chemistry.

(Burton and others, 1951; Uwaha, 2016), and in general is widely applied to any reactions involving crystal surfaces (Jansen, 2012).

Blum and Lasaga (1987) developed dissolution models in the presence of crystal defects, for example screw dislocations. They used the commonly accepted expression for the dissolution rate given as:

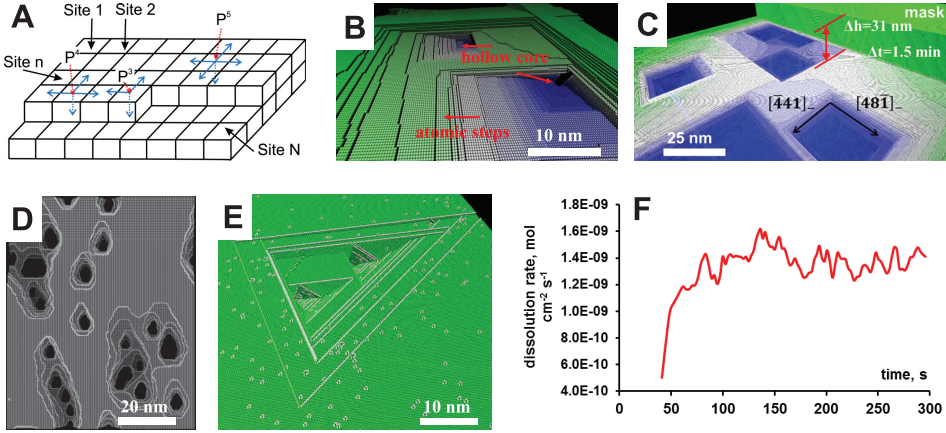$$k_i = \nu \, exp\left(-i\,\frac{E}{kT}\right), \tag{8}$$

Fig. 3. Kinetic Monte Carlo simulations of mineral dissolution. (A) A cubic Kossel model with N surface sites and five dissolution probabilities defined by site coordination. (B) Simulated surface of calcite with steps emanating from dislocation hollow cores. (C) Normal surface retreat relative to a non-reactive mask, calcite crystal with screw dislocations. (D) Pitted surface of phlogopite. (E) Surface of quartz rhombohedral face and two dislocations. (F) Dissolution rate of calcite in material flux units, simulations. B,C,F are reprinted (adapted) with permission from (Kurganskaya and Luttge, 2016). Copyright (2016) American Chemical Society. B-E are produced by using VMD software (Humphrey and others, 1996).

where ν is the frequency factor, assumed to be universal for simplicity, i is the number of bonds to be broken, E is the activation barrier, kT is the Boltzmann factor. Wehrli (1989) used the same approach to simulate dissolution of solid oxides surfaces without dislocations. The dissolution probabilities can be easily calculated from (eq 7) and (eq 8):

$$P_i^- = \frac{1}{\sum_{i=1}^{6} N_i exp\left(-\frac{i\Delta E_a}{kT}\right)} N_i exp\left(-\frac{i\Delta E_a}{kT}\right) = \frac{1}{Q}N_i exp\left(-\frac{i\Delta E_a}{kT}\right),$$ (9)

where ΔE_a is the activation energy of M-O-M bond breaking, i is the number of nearest neighbors (fig. 3A), N_i is the number of sites with i bonds. As it can be easily noted from the (eq 9), the probabilities change with every change of surface configuration. The time increment Δt corresponding to a reactive transition depends on the value of the pre-factor in the (eq 9):

$$\Delta t = \frac{1}{\nu Q}\ln(r),$$ (10)

where r is a random number (Voter, 2007). The $\ln(r)$ term is frequently omitted for better convergence of the algorithm, since statistically it converges to the same solution (Boerrigter and others, 2004). Since populations of different reactive sites may change at a new iteration step, the time step is not constant. At every iteration step a reactive transition is performed. This algorithm thus provides a computationally efficient scheme to propagate the system through time. The algorithm was developed by Bortz, Kalos and Lebowitz as a fast rejection-free alternative to the Metropolis "rejection-acceptance" algorithm and is known in the literature as BKL (Bortz and others, 1975) or "divide-and-conquer" algorithm (Meakin and Rosso, 2008).

Since defects generate distortions in the crystal lattice, the corresponding stress fields can be calculated from the linear elasticity theory (Hull and Bacon, 2011). The

strain energy changes probability of atom dissolution, as a result, etch pits and tubes open in the beginning of the dissolution process (Honess, 1927; Blum and Lasaga, 1987; Lasaga and Luttge, 2001; Meakin and Rosso, 2008). These features generate atomic steps on the surface (fig. 3B), which movement results in surface normal retreat Δh (fig. 3C) (Lasaga and Luttge, 2001) that can be measured as a difference in mean surface heights for reacted and unreacted ("masked") surfaces. This approach is used in mineral dissolution experiments where surface topography can be directly measured (Luttge and Arvidson, 2010). This surface normal retreat corresponds to the material loss rate that can be measured in material flux units moles $\cdot$ cm^{-2}s^{-1}. The quantitative relationship between surface normal retreat and material flux is straightforward (Luttge and Arvidson, 2010):

$$R = V_m^{-1} \frac{\overline{\Delta h}}{\Delta t}, \tag{11}$$

where V_m^{-1} is the inverted molar volume of a mineral, $\overleftarrow{\Delta h}$ is the surface normal retreat measured as an average height difference, Δt is the corresponding time interval.

The model was extended further and tested for different types of defects, for example point defects, screw and edge dislocations, and extended system sizes allowing multiple etch pits to form (Meakin and Rosso, 2008). KMC models simulating dissolution process at the etch pits and atomic steps were applied to understand dissolution kinetics of minerals as a function of their chemical composition and lattice structure, for example carbonates (Kurganskaya and Luttge, 2016), feldspars (Zhang and Lüttge, 2007; Zhang and Lüttge, 2008; Zhang and Lüttge, 2009a), fluorite (Cama and others, 2010), phyllosilicates (fig. 3D) (Kurganskaya and Luttge, 2013a) and quartz (fig. 3E) (Kurganskaya and Luttge, 2013b). The KMC simulators do not only produce surface topographies and etch pit structures, but also provide statistics of site distributions and time-dependent material flux from the surface (fig 3F). The dissolution rate in the flux units can be calculated from KMC simulations by restricting a part of a surface from reactions (creating a digital "mask") and using (eq 11). A straightforward approach is to count the number of dissolved molecules over a time period (eq 10) and dividing by the lateral area of a simulated surface (fig. 3F):

$$R = N_A \frac{1}{A} \frac{\Delta N}{\Delta t}, \tag{12}$$

where ΔN is the number of dissolved atoms normalized by mineral stoichiometric formula, N_A is Avogardo's number, A is the geometric area of a simulated surface.

Dissolution of grains, especially nanograins, may exhibit totally different kinetic behavior (Zhang and Lüttge, 2009b) not related to dislocations. Grain corners and edges are defect sites supplying the surface with atomic steps, that may override influence of dislocations, and generate circular steps dominating the surface (Briese and others, 2017). Dissolution process at nanoconfined conditions is another interesting effect studied by a KMC method (Høgberget and others, 2016) – the limited material transport and competition between dissolution and growth may result in formation of dissolution cavities (Kohler and others, 2018). These results clearly show that behavior of nanoconfined fluids and solids may follow size-specific dissolution mechanisms.

The overall dissolution mechanism for minerals is system-specific and depends on crystal structure, arrangement of bonds at a specific crystal face as well as structure of interface water and distribution of adsorbed ions, distribution of lattice defects, grain size and morphology. For confined systems, the material transport starts to play a significant role. The primary role of the lattice defects is to provide sources of the

reactive features, such as atomic steps. The crystallographic direction of the steps, their velocities and superposition at the surface define etch pit morphology and dissolution mechanism. If a KMC model incorporates all kinetically relevant reaction controls (see further text regarding parameterization), these mechanisms will manifest themselves in the output data. An important step is identification of the potential stable step and kink sites at a given crystal face. This can be done via topological analysis of lattice bonding network (Grimbergen and others, 1998; Meekes and others, 1998; Grimbergen and others, 1999), for example, by using dedicated software such as ToposPro (Blatov and others, 2014; Anderson and others, 2017).

Atomistic-KMC models connection.—KMC algorithm works as a stochastic event scheduler, where reactive events and their rates are required as input parameters. The construction of proper reactive event's list characterized by correct rates is the step necessary to produce a correct KMC model. Quantum mechanical and Molecular Dynamics calculations may provide important information about reaction rates and rate-controlling mechanisms. Ideally, all possible reactions and rates at all possible surface configurations should be calculated. In most cases this goal is not achievable due to excessively large number of possible reactions. Further we consider different parameterization approaches based on the atomistic modeling.

Heuristic parameterization.—In the case of obscure reaction controls and mechanisms at the molecular scale, the parameterization process can be used as a non-trivial hypothesis testing tool. Dissolution process at each surface site can be in principle characterized by the key rate-controlling factors found from QM/MD calculations. The functional influence of these factors onto the analytical expressions for rates/probabilities is a subject of evaluation, but in general it is assumed to be a linear combination of energetic parameters. In the case of solid solutions, for the example the plagioclase series, parameterization is straightforward:

$$P_{ij}^- = \frac{N_{ij}}{Q} exp\left(-\frac{i\Delta E_{Si-O-Si} + j\Delta E_{Si-O-Al}}{kT} \right), \tag{13}$$

where i is the number of Si-O-Si and j is the number of Si-O-Al neighbors. The difference in activation energies for Si-O-Si and Si-O-Al bond breaking combined with the cation order-disorder properties results in the rate variance for plagioclases with fixed chemical composition (Zhang and Lüttge, 2007; Zhang and Lüttge, 2008; Zhang and Lüttge, 2009a). The same parameterization approach was applied to Al-Si phyllosilicates, where a reactive center can be characterized by ijk triplets, where i is the number of tetrahedral Si neighbors, j is the number of tetrahedral Al neighbors, k is the number of octahedral Al neighbors (fig. 4A) (Lasaga, 1995; Kurganskaya and Luttge, 2013a).

The influence of the bond topology on bond hydrolysis activation energies found from QM studies (Pelmenschikov and others, 2000) leads to the essential dependence of probabilities on the number of neighbors in the second coordination sphere. Incorporation of the second-order neighbor influence into the KMC model of muscovite dissolution (fig. 4B) (Kurganskaya and Luttge, 2013a) resulted in reproducibility of all (hk0) faces observed in AFM experiments (figs. 4C-4E) (Kurganskaya and others, 2012). The mechanistic explanation lies in bond topology-based distinguishability of step and kink sites at certain (hk0) faces. The same principle was adopted to simulate dissolution of quartz faces: rhombohedral, prism, and pinacoid. The parameterization approach and values of the parameters showed a clear influence onto morphology of the dissolution features, and surface topographies for prism and pinacoid faces (fig. 5) (Kurganskaya and Luttge, 2013b).

Energetic barriers and pre-factors.—Reactive systems that are well-studied at the atomistic level can be parameterized with the TST rate constants (eq. 6) obtained from
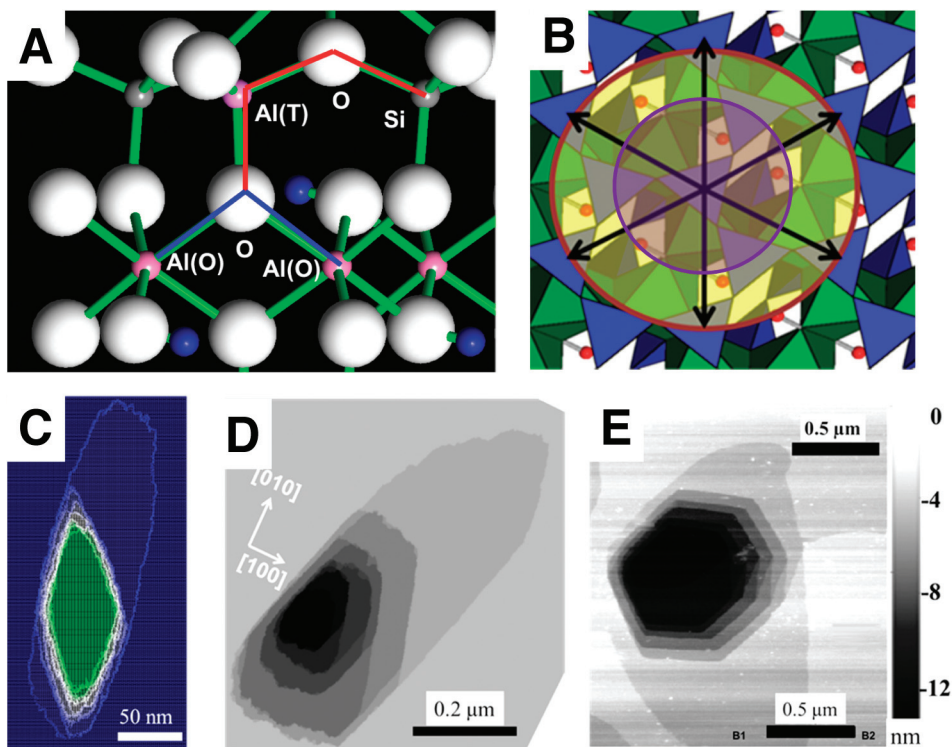
Fig. 4. Kinetic Monte Carlo simulations of muscovite dissolution (Kurganskaya and Luttge, 2013a). (A) Chemical bonds in muscovite lattice; (B) First (purple circle) and second (red circle) coordination spheres of a tetrahedrally coordinated atom in muscovite; (C) Etch pit obtained from first coordination sphere model; (D) Etch pit obtained from second coordination sphere model; (E) Etch pit obtained from Atomic Force Microscopy measurements. Reprinted from (Kurganskaya and Luttge, 2013a), Copyright (2013), with permission from Elsevier.

ab initio/MD studies as we discussed in the *Molecular Dynamics section*. In this case, the total rate list of the kinetically relevant reactions can be constructed and the KMC program can be supplied with the molecular rate constants as input parameters. Direct calculations of the TST rates for every reaction in the system are computationally expensive and typically are not provided. Instead, reaction barriers are more often found in literature. The majority of KMC models exploit the following semi-empirical equation relating rate and energetic barrier:

$$k = \nu\, e^{-\frac{E}{kT}}, \qquad (14)$$

where ν is the reaction attempt frequency, $e^{-\frac{E}{kT}}$ is the probability of reaction occurrence, E is the value of the activation barrier. In the reactive collision theory, the pre-factor is the number of collisions multiplied by the steric factor. Since surface reactions have much more complex dynamics and the exact value of the pre-factor is not easy to calculate, the atomic vibrational frequency is used. Thus, Pelmenschikov and others (2001) used water vibration frequency of 10^{12} Hz to approximate ν for dissolution, and 10^{13} Hz of Si-OH bond vibration frequency for atomic attachment. Chen and others (2014) simulated dissolution of NaCl by using activation barriers obtained from the DFT studies and lattice vibration frequencies as pre-factors. Lasaga
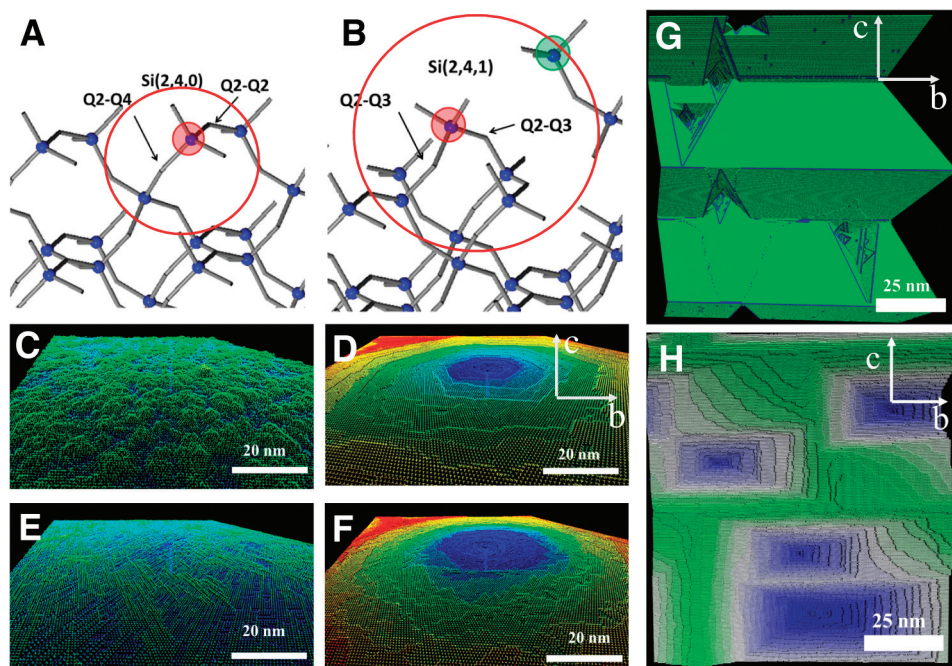
Fig. 5. Kinetic Monte Carlo simulations of quartz dissolution (Kurganskaya and Luttge, 2013b). (A),(B) Si-O-Si bonding network, Qi-Qj denotes bond topology (number of nearest neighbors at bond-forming Si sites), Si(n,m,l) denotes Si sites with the predefined dissolution rates depending on n first order neighbors, m second order connected neighbors and l second order disconnected neighbors. (A) First coordination sphere, (B) Second coordination sphere. C-F. KMC simulations of pinacoid (001) face dissolution. (C) First coordination sphere model, FCS. (D) Second coordination sphere (SCS) model (connected and disconnected neighbors are indistinguishable), (E) SCS model excluding disconnected second order neighbors from bonding interactions; (F) SCS model assigning "weak" interactions with disconnected second order neighbors. G,H. Prism (100) face, (G) FCS model; (H) SCS model. Reprinted (adapted) with permission from (Kurganskaya and Luttge, 2013b). Copyright (2013) American Chemical Society.

and coworkers assumed a constant pre-factor value for all surface reactions and omitted it from the probability equations (Lasaga and Blum, 1986; Blum and Lasaga, 1987).

The community of scientists studying catalytic surface reactions in vacuum (see methodological outline in Jansen, 2012) is commonly using pre-factors derived from the statistical mechanics of gas-surface reactions in Langmuir systems (Pitt and others, 1995). This "fully *ab initio*" approach can be used to identify rate-limiting steps in surface catalysis, for example HCl oxidation on RuO_2 surface (Hess and Over, 2017), or to predict surface film growth on degrading lithium-ion batteries (Röder and others, 2017). Derivation of the partition functions for the complex many-body systems such as mineral surface, fluid and interface species in general form is challenging and has not been done so far. Therefore, the most promising approach at the moment is the calculation of the rates based on free energies and transmission coefficients (eq 4, eq 6) obtained from MD simulations.

"Direct coupling" parameterization.—Molecular dynamics simulations are time dependent. In the case of relatively fast reactions happening during the simulation run, the rates can be calculated by directly counting the numbers of dissolution and precipitation events from all sites with different bonding environments. Piana and Gale followed this approach to collect statistics on such transitions for urea crystals and

classify the sites based on the difference in rates (Piana and Gale, 2005). These data were used in the KMC model simulating growth of urea crystals (Piana and Gale, 2006). A perfect match between experimentally measured and calculated growth rates and crystal morphologies was shown (Piana and others, 2005).

Grand Canonical Monte Carlo

The grand canonical monte Carlo method is widely used to simulate open systems with constant volume, temperature and chemical potentials (μ,V,T) (Frenkel and Smith, 2002). This powerful method can be applied to a large variety of systems, where particles, for example ions and molecules, can be explicitly used as interacting species. The GCMC method was applied to simulate mineral surface charging processes, in the absence and presence of electrolytes (Labbez and others, 2006; Labbez and Jönsson, 2006), capture effects of charged site geometric position onto their acidity properties (Sulpizi and others, 2012). The method is based on the Metropolis Monte Carlo algorithm: trial moves are generated randomly and the probabilities based on the energetic differences between the old and new states are calculated. The transition is accepted if the value of a random number is less than the probability calculated from a Boltzmann distribution defined for a system of interest. The surface sites can be defined as immobile particles where protonation and deprotonation reactions may occur. Ions move freely in the simulation box and may adsorb on the surface, thus creating electric double layer characterized by zeta potential measured in experiments (Churakov and others, 2014).

KMC-GCMC model.—The GCMC method is developed to sample out the system's configurations at the equilibrium (μ,V,T) ensemble. The equilibrium concept is applied to thermodynamic equilibrium with external reservoir. The process of the proton exchange on the surface, as well as motion of hydrated ions around the interface, normally happens much faster than processes of atomic detachment/ attachment via chemical bonding. In such a scenario, the system can be in the equilibrium with respect to protonation and ion diffusion, but not in the equilibrium with respect to the solid state where dissolution reactions occur. Protonation of the surface sites and ion adsorption may significantly change the hydrolysis reaction mechanism and rate. The information about site type protonation and ion adsorption probability provide a valuable kinetic information. A combination of Kinetic Monte Carlo and GCMC approaches was successfully applied to understand mechanisms of pH dependence of carbonate dissolution in the presence of electrolytes (Kurganskaya and Churakov, 2018).

GCMC simulations were used to obtain quantitative information about populations of protonated sites as a function of pH and electrolyte concentration. Site acidity constants (pK_a) calculated from *ab initio* MD simulations (Andersson and Stipp, 2012) were used as input parameters for GCMC model. GCMC simulations of pitted carbonate surfaces (fig. 6A) revealed clear dependence of site acidity on its coordination as well as on presence of electrolytes (figs. 6B and 6C). Comparison of simulated and experimentally observed pit structures (figs. 6D and 6E), combined with analysis of material flux pH-dependence (fig. 6F) revealed the most probable mechanisms at specific pH-ranges: at pH=9-12 protonation of kink sites is responsible for the linear pH-dependence, at pH=5-9 protonation of step sites generate the dependence while most of kink sites are protonated, at pH=2-5 double protonation and conversion of surface carbonate into CO_2 of surface sites is responsible for the linear pH-dependence (Kurganskaya and Churakov, 2018).

Experimental observations: verification and parameterization of the KMC and GCMC models.—Experimental studies of mineral dissolution mechanisms and rates are the only way to validate KMC models. Atomically resolved geometries of etch pits provide an incredibly detailed source of kinetic information regarding relative reactivities of
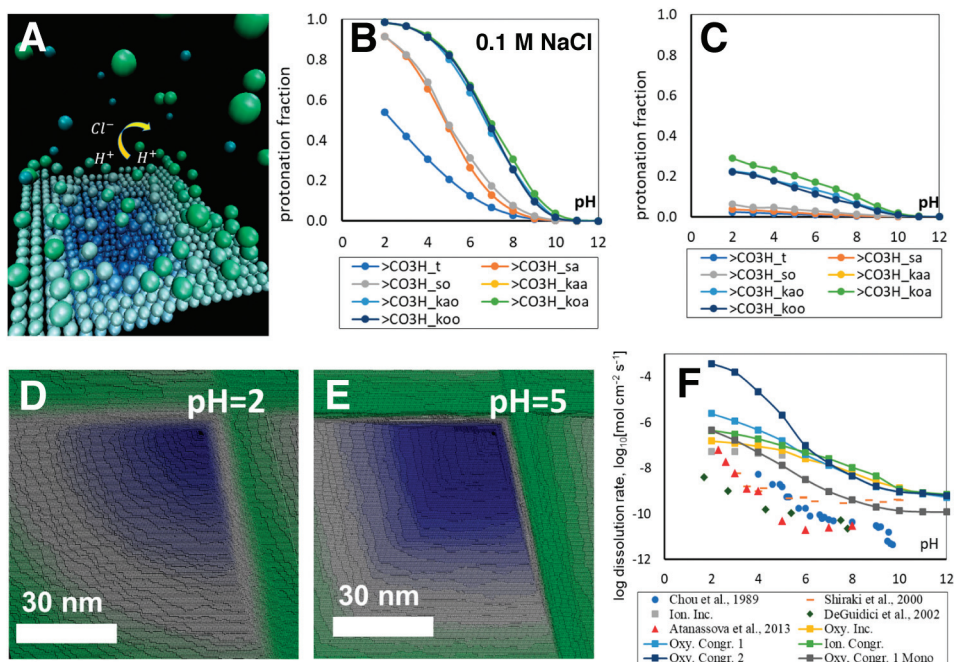
Fig. 6. Grand Canonical Monte Carlo (GCMC) and Kinetic Monte Carlo (KMC) simulations used to obtain chemical dependencies of dissolution rates (Kurganskaya and Churakov, 2018). (A) Calcite surface with etch pit and ions used in GCMC simulations. (B) Fractions of protonated sites as a function on pH in the presence of 0.1M NaCl. (C) Protonation fractions in the absence of electrolytes. (D,E) Etch pit structures obtained in KMC simulations, at pH=2 and pH=5. (F) Dissolution rates as a function on pH, compilation of published experimental data and KMC simulations. Reprinted (adapted) with permission from (Kurganskaya and Churakov, 2018). Copyright (2018) American Chemical Society.

atomic steps moving in different crystallographic directions. This information can be obtained from measurements of surface topography, for example Atomic Force Microscopy (AFM), Vertical Scanning Interferometry (VSI), or surface imaging techniques, for example, Secondary Electron Microscopy (SEM). Large amount of data is accumulated from the AFM measurements. Pitted surface topographies were obtained for a wide range of minerals, for example phyllosilicates (Rufe and Hochella, 1999; Aldushin and others, 2006a; Aldushin and others, 2006b; Shao and others, 2011), quartz (Gratz and others, 1991; Gratz and Bird, 1993b; Gratz and Bird, 1993a; Yanina and others, 2006), fluorite (Cama and others, 2010; Motzer and Reichling, 2010),carbonates (Hillner and others, 1992; Liang and others, 1996; King and Putnis, 2013; Klasa and others, 2013; Offeddu and others, 2014). Vertical Scanning Interferometry can be used for direct systematic measurements of dissolution rates via surface normal retreat, observations of a large variety of dissolution scenarios and surface topographies (Arvidson and others, 2003; Vinson and others, 2007; Luttge and Arvidson, 2010; Atanassova and others, 2013; Daval and others, 2013; Emmanuel, 2015; Pollet-Villard and others, 2016; Michaelis and others, 2017; Noiriel and others, 2018). All these data are necessary to verify KMC models in terms of their predictive ability of etch pit and surface structures (Cama and others, 2010; Kurganskaya and Luttge, 2013a) as well as dissolution rates (Kurganskaya and Luttge, 2016). Chemical conditions may affect dissolution mechanisms. Influence of pH conditions onto step velocities had been demonstrated using AFM (Shiraki and others, 2000; Giudici, 2002; Duckworth and

Martin, 2004), as well as influence of the background electrolytes (Ruiz-Agudo and others, 2010; Klasa and others, 2013). These data can be used to obtain parameters for the KMC-GCMC models (Kurganskaya and Churakov, 2018). Verification of the rate pH-dependencies can be obtained from the macroscopic measurements of rates in single crystal or powder experiments [that is, for calcite (Chou and others, 1989; Shiraki, and others, 2000; Giudici, 2002; Duckworth and Martin, 2004)]. The direct comparison is problematic due to the difference in the system sizes and associated intrinsic rate variance (Lüttge and others, 2013). However, the major pH trends still can be verified, although they also can be modified by the influence of the fluid chemistry variations that can be hard to avoid in experimental settings (Colombani, 2016).

The problem of the intrinsic rate variance (several orders of magnitude) measured at identical chemical conditions substitutes a serious fundamental challenge in upscaling any results of the KMC models to macroscopic systems. The major obstacle is the poor definition of the reactive systems in terms of the reactive site sources, for example, etch pits, grain edges, *et cetera* (Arvidson and others, 2003; Fischer and others, 2012; Lüttge and others, 2013; Fischer and others, 2014). The clear advantage of the KMC approach is the ability to relate directly local surface morphologies, reactive site statistics, material fluxes and surface normal retreat (Kurganskaya and Luttge, 2016).

In general, the most efficient approach to elucidate reaction mechanisms and kinetics is the combination of atomistic modeling studies with experimental data. KMC model then serves as a universal tool allowing us to identify kinetic steps controlling surface morphology and the overall rate. The community of surface scientists studying catalytic gas-surface reactions has much bigger database of DFT/MD derived energetic barriers and rates then the geoscience community. Remarkably, they came to the same conclusion regarding KMC model parameterization (Exner and others, 2015; Hess and Over, 2017). KMC thus serves as a ubiquitous statistical mechanics tool capable to discover new information about possible surface site and reactive feature configurations as well as to define bottleneck processes that can be further used to develop new kinetic theories.

Reactive Canonical Monte Carlo

An alternative technique, designed for simulations of the equilibrium solid-fluid systems, is the Reactive Canonical Monte Carlo (RxCMC) where the number of species is fixed and there is no chemical potential involved. The bonds can break and form between the molecules, thus allowing reactive transitions between the species in the system. The transition probabilities depend on the energetic difference between the old and the new states:

$$P_{old \rightarrow new} = e^{-\beta(U_{new} - U_{old})} \prod_{i=1}^{c} q_i^{v_i} \prod_{i=1}^{c} \frac{N_i!}{(N_i + v_i)!}, \tag{15}$$

where U denotes the system's potential energy calculated from an appropriate force field, q_i, N_i and v_i are the partition function, number and stoichiometric coefficient for an ith specie (Johnson and others, 1994). Nangia and Garrison used this method to study quartz-water interaction at equilibrium conditions (Nangia and Garrison, 2009). Since the kinetics are not incorporated into this modeling algorithm based on the pure statistical mechanics, the model provides the statistics from the configurational space sampling with respect to "dissolution" and "precipitation" moves for the closed system at chemical equilibrium. They tested two different statistical models: (1) with the stepwise bond breaking events; (2) with the direct removal of two- and – three bonded sites. They reported that the direct removal of these sites is the more probable dissolution mechanism than the step-wise bond breaking. They used the same approach to

calculate relative stability and dissolution mechanisms of different cristobalite planes at equilibrium conditions (Nangia and Garrison, 2010).

Analytical Models of Step Kinematics

The analytical models of crystal dissolution and growth are aimed at providing a mechanistic picture of the process coupled with the quantitative prediction of the process rates. A historically important paper that gave rise to the numerous studies in this field is written by Burton, Cabrera and Frank (Burton and others, 1951) commonly referred to as "the BCF theory". In this paper the growth of monomolecular crystals from vapor is explained as the process of atomic attachment at the kink sites as a function of solution concentration, temperature and other parameters. The detailed derivation from the prospective of the statistical mechanics is provided. The kink sites were demonstrated as primary surface sites controlling atomic step advancement and growth kinetics. The models of crystal dissolution commonly incorporate three primary steps: kink site formation, propagation and annihilation. Zhang and Nancollas derived kink densities at non-equilibrium conditions based on these processes (Zhang and Nancollas, 1990) and extended this model to the case of an AB crystal in nonstoichiometric solution (Zhang and Nancollas, 1998). Stack and Grantham and Bracco and others (Stack and Grantham, 2010; Bracco and others, 2012) developed a model of step kinematics based on a similar approach, by considering kink site attachment, detachment and nucleation events for the model of calcite growth. They provided estimates for the rates of these events by fitting step velocities to their experimentally measured values. Wolthers and others (2012) applied this model to explain dependence of calcite step velocities on the ratio of calcium and carbonate ions in the fluid. They constructed a detailed pH-dependent model incorporating protonation and deprotonation reactions. The model contains a large number of parameters that authors constrained with experimentally measured step velocities, theoretical calculations and approximations. Nielsen and others (Nielsen and others, 2012) used the same approach based on Zhang and Nancollas model (Zhang and Nancollas, 1998) to calculate ionic attachment frequencies and to construct a mechanistic model of isotope and trace element fractionation during calcite growth. These models provide the quantitative relationships between the event statistics at the atomic scale and step kinematics. Another family of models developed by Chernov, DeYoreo, Dove, Vekilov and others is dedicated to the relation of the step kinematics to the thermodynamic and geometric parameters, for example, saturation state, surface free energy, step length and curvature (Chernov, 1961; De Yoreo and Vekilov, 2003; Dove and others, 2005; De Yoreo and others, 2009).

A novel promising approach relating the Transition State Theory and step kinematics from the rigorous statistical mechanics point of view has been developed (Li and others, 2016; Tilbury and others, 2017). The authors constructed a detailed model of step propagation based on the step-wise processes of molecule desolvation and attachment, thus connecting directly MD derived molecular reaction mechanisms and atomic step advancement.

The expressions for the step velocities as functions of environmental conditions provide a possibility to upscale the dissolution and growth rates. Current approach to upscale by assuming constant step density (Bracco and others, 2013) seems to be problematic due to the heterogeneous distributions of steps and etch pits commonly occurring on mineral surfaces. Modeling of the spatial step and etch pit distribution thus becomes an important step in providing a connection between the models based on the statistical mechanics description of the atomistic processes and continuum and pore scale reactive transport models.
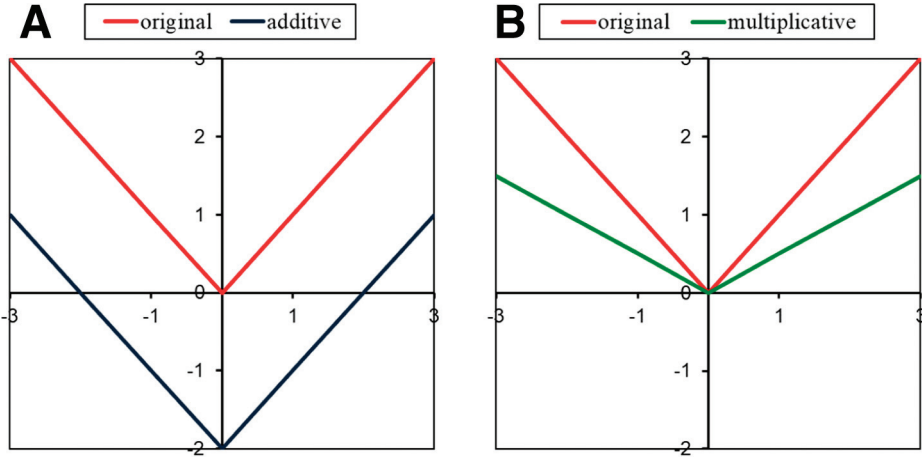
Fig. 7. Weighting of etch pits for a Voronoi surface model by using (A) Additive weighting; (B) multiplicative weighting (see explanation in the text).

Voronoi Models

Voronoi diagrams are a geometrical concept that originated in the mathematical works of Dirichlet (Dirichlet, 1850) and Voronoi (1908a, 1908b). Conceptually, a space S consisting of a set M and a relationship (distance function) D is partitioned into regions usually called *cells,* based on a subset of generating points from that space, and the *distances* of all other points to the generating points. A Voronoi cell around the generating point P is the subset of the points of M that are closer to P than to any other generating point. The Voronoi diagram itself is defined as the subset of M whose members have the same distance to at least two generating points.

Distance, in this case, is not limited to the Euclidean distance but can refer to any distance function whatsoever. Also, the generating points can be *weighted,* additively or multiplicatively, which means that the distances to a generating point are manipulated by adding something to them or multiplying them with a number. (Fig. 7) shows a 2-dimensional example of additive and multiplicative weighting process. The original pit represents the unweighted case of a simplified etch pit cross section, using the distance function

$$D(x) = |x| \tag{16}$$

which generates an "etch pit" with completely straight walls.

Using additive weighting is shown in (fig. 7A). A weighting factor of 2 is subtracted from all the distances, resulting in the formula

$$D_{add}(x) = |x| - 2 \tag{17}$$

which shifts the etch pit downwards, making it deeper.

Multiplicative weighting is done by dividing the original values by the weighting factor. (Fig. 7B) shows multiplicative weighting, using also a weighting factor of 2, with the formula

$$D_{mul}(x) = |x|/2 \tag{18}$$

which changes the slope of the etch pit walls.

A comprehensive review of the resulting data structures can be found for example in Aurenhammer's review (Aurenhammer, 1991) and citations therein.

We have been using non-Euclidean weighted Voronoi diagrams for the simulation of a dissolving Kossel crystal surface (Rohlfs and others, 2018). We considered a flat starting surface the space we're operating on, and the outcrops of screw dislocations (for simplicity's sake assumed to be infinitely long and perpendicular to the surface) the generating points of our Voronoi distance map.

The non-euclidean distance we used in this case is the maximum norm, which was chosen due to generating square isolines. Since with sufficiently high bond strength the etch pits generated on a Kossel crystal face have square shape, this norm was considered a reasonable basis for geometrical modeling.

The surface height at a certain point after a dissolution time t was then described as a function of distance r to the nearest defect. The distance r is defined by the maximum norm, calculating the directional distances in x and y directions and then choosing the larger of those two values as the distances. We used step velocities according to the stepwave model (Lasaga and Luttge, 2001) and derived from that first the arrival time *arr(r)* as

$$arr(r) = \frac{r_{crit} \times \ln(r - r_{crit}) + r}{v_{step}} \tag{19}$$

[see (Rohlfs and others, 2018)] and then the height as

$$H(r,t) = H_0 - ((t - arr(r)) \times v(r_{pit})) \tag{20}$$

[also see (Rohlfs and others, 2018)] with H_0 being the starting height and (r_{pit}) being the global retreat rate. This gives the height as a function of distance, time and step velocities.

To take into account the heterogeneity of etch pit depth evolution, additive weighting of this distance function was used. Some etch pits were assigned a high weighting factor to account for deeper growth in the same amount of time in which other etch pits were less active. In our 2018 study (Rohlfs and others, 2018) we used weighting factors directly derived from etch pit depths in kMC simulations to make the calculations directly comparable with kMC-generated surfaces. It is however also possible to draw weighting factors from synthetic distributions, whose statistics are currently being investigated.

The calculation of surface heights and subsequent construction of height maps directly from the stepwave model provides a link between the reaction kinetics and computational geometry. This is important from the theoretical standpoint as a validation of the modeling approach, since mere correlation would not be enough to consider a model useful. The generated data not only look very similar to data generated with other methods [see (fig. 8)] but are actually consistent with our current understanding of dissolution kinetics.

KMC-Voronoi models connection.—The distance function used for simulating the system is strongly dependent not only on the crystal lattice, which determines the shape and symmetry of the distance function iso lines, but also the bond strength and other environmental factors. Information about these details cannot come from the Voronoi simulations but is required as input. In this case, we parameterized the Voronoi model with data gained from the Kinetic Monte Carlo (KMC) simulations. For details about the various parameters and their connection to KMC models see Rohlfs and others (2018). We then compared the generated data in terms of material flux and surface roughness parameters.
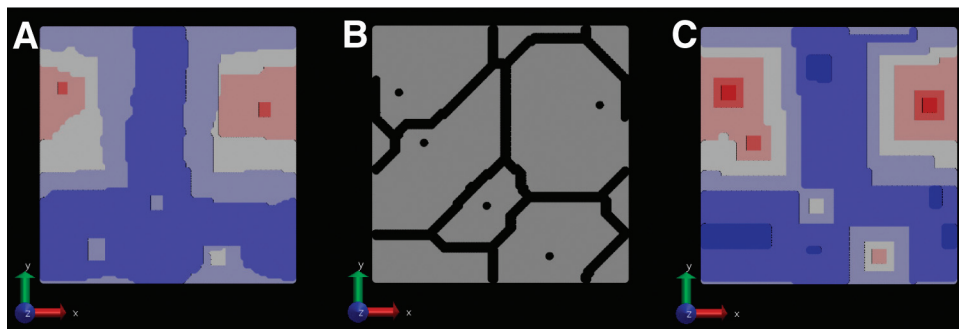
Fig. 8. 100x100 atoms, periodic boundary conditions, 5 screw defects. (A) kMC simulation of 500000 removed atoms. (B) Weighted Voronoi diagram using defect positions as generating points, and weighting factors gained from the kMC simulation. (C) Reconstructed Voronoi distance map using system-specific distance function. Images generated with VMD software (Humphrey and others, 1996).

The modeling results clearly show that there is a geometrical relationship between defect positions and the heterogeneous dissolution of a crystal surface.

It should be noted that other, less symmetrical crystal structures can also be simulated with Voronoi methods. The anisotropy can be taken into account by using an accordingly modified distance function.

In (fig. 8), the approach is illustrated. The stochastically generated kMC simulation is reduced to its underlying data structure, a weighted Voronoi diagram. This, in combination with a non-Euclidean distance function specific to the system, can reconstruct the surface morphology with sufficient accuracy. The Voronoi calculation cannot simulate small-scale details, for example atomic step structure or spontaneously occurring non-defect driven monolayer etch pits. It can, however, reflect the overall reactivity distributions observed on the dissolving surface. Coalescence of neighboring etch pits requires special methodological approach, as described in Rohlfs and others (2018).The obvious advantages of using a simulation method based on computational geometry are faster computational speed and low computational requirements. Indeed, it is possible to carry out simulations on an ordinary laptop computer and to handle larger systems than those that are currently being handled with kMC.

However, the main justification of the method we see in its potential for upscaling. The possibility to construct correctly surface morphology based on a limited number of parameters and simple analytical scale-independent functions is a great opportunity to filter kinetically relevant information. It implies that, for a known system under known conditions, the development of morphology and roughness can at least initially be described by the distribution function of weighting factors. This makes Voronoi simulations an efficient tool for data reduction.

Future aim is to use this advantage to combine Voronoi methods with larger-scale fluid dynamics and Lattice Boltzmann simulations.

CONCLUSIONS AND PROSPECTS

Modern computer era enables a unique possibility for the geoscience community to study mineral-water interactions in all mechanistic details and cover all spatial and temporal scales. Quantum Mechanical and Molecular Dynamics methods reproduce chemically and physically correct atomistic details of the dissolution process, involving bonding interactions between crystal and water molecules, as well as bond breaking and formation processes. Chemical complexity of the mineral-water interface structure at the molecular level and large number of possible reactions can be efficiently

managed by using the stochastic Kinetic Monte Carlo approach. KMC models require input data in the form of reaction lists and reaction rates. The latter ones can be obtained from QM/MD calculations. The simulation results can be verified by experiments. Environmental parameters defined by the fluid phase in the form of pH, ionic concentrations and other chemical details, at the molecular level change mineral-water interface structure. Quantitative statistical description of such changes in terms of distributions of protonated/deprotonated sites and adsorbed species can be obtained from the Grand Canonical Monte Carlo simulations. A combination of KMC and GCMC methods allows us to quantitatively study dependencies of the dissolution rates on fluid chemical composition. Analytical predictions of surface topography from Voronoi partitioning based on geometric arrangements of defect distributions constitute a new promising quantitative technique. Use of this method in a combination with atomistic KMC models enables compact convolution of these models into larger scale kinetic solvers that can be applied for pore-scale dissolution/precipitation phenomena coupled with reactive transport.

The geochemical community nowadays is facing a challenging task: the development of a consistent methodological and theoretical framework for mineral dissolution studies covering all scales at all geologically and environmentally relevant conditions. Top-down approach to derive molecular mechanisms from macroscopic observations is methodologically challenging especially for complex geochemical systems. The bottom up approach seems to be promising in its predictive capability, but the complexity of the system is growing tremendously quickly with the system size. A critical milestone problem is then the development of methodological and theoretical interfaces stitching different scales. This would require us, as the community, to critically evaluate the up-to-date knowledge acquired from numerical simulations, analytical, statistical and stochastic models, as well as experimental observations, with respect to its consistency and mutual compatibility. The next step would require us to develop a new generation of analytical and numerical models, relevant parameters and protocols for experimental data acquisition and data analysis. The ultimate goal is to turn the "*terra incognita*" of loosely-defined chemical systems in mineral dissolution kinetics into an exact science operating physically well-defined variables, dependencies, parameters and processes, quantitatively consistent at all hierarchical levels.

REFERENCES

Aldushin, K., Jordan, G., and Schmahl, W. W., 2006a, Basal plane reactivity of phyllosilicates studied *in situ* by hydrothermal atomic force microscopy (HAFM): Geochimica et Cosmochimica Acta, v. 70, n. 17, p. 4380–4391, https://doi.org/10.1016/j.gca.2006.04.015

—— 2006b, Kinematics of apophyllite leaching—A terrace–ledge–kink process within phyllosilicate interlayers: Journal of Crystal Growth, v. 297, n. 1, p. 161–168, https://doi.org/10.1016/j.jcrysgro.2006.08.042

Allen, M. P., and Tildesley, D. J., 2017, Computer Simulation of Liquids: Oxford, United Kingdom, Oxford University Press, https://doi.org/10.1093/oso/9780198803195.001.0001

Anderson, M. W., Gebbie-Rayet, J. T., Hill, A. R., Farida, N., Attfield, M. P., Cubillas, P., Blatov, V. A., Proserpio, D. M., Akporiaye, D., Arstad, B., and Gale, J. D., 2017, Predicting crystal growth via a unified kinetic three-dimensional partition model: Nature, v. 544, p. 456–459, https://doi.org/10.1038/nature21684

Andersson, M. P., and Stipp, S. L. S., 2012, How acidic is water on calcite?: The Journal of Physical Chemistry C, v. 116, n. 35, p. 18779–18787, https://doi.org/10.1021/jp304671k

Arvidson, R. S., Ertan, I. E., Amonette, J. E., and Luttge, A., 2003, Variation in calcite dissolution rates:: A fundamental problem?: Geochimica et Cosmochimica Acta, v. 67, n. 9, p. 1623–1634, https://doi.org/10.1016/S0016-7037(02)01177-8

Atanassova, R., Cama, J., Soler, J. M., Offeddu, F. G., Queralt, I., and Casanova, I., 2013, Calcite interaction with acidic sulphate solutions: A vertical scanning interferometry and energy-dispersive XRF study: European Journal of Mineralogy, v. 25, n. 3, p. 331–351, https://doi.org/10.1127/0935-1221/2013/0025-2279

Aurenhammer, F., 1991, Voronoi Diagrams—a Survey of a Fundamental Geometric Data Structure: ACM Computing Surveys, v. 23, n. 3, p. 345–405, https://doi.org/10.1145/116873.116880

Blatov, V. A., Shevchenko, A. P., and Proserpio, D. M., 2014, Applied Topological Analysis of Crystal Structures with the Program Package ToposPro: Crystal Growth & Design, v. 14, n. 7, p. 3576–3586, https://doi.org/10.1021/cg500498k

Blum, A. E., and Lasaga, A. C., 1987, Monte Carlo simulations of surface reaction rate laws, *in* Stumm, editor, Aquatic surface chemistry: Chemical processes at the particle-water interface: New York, Wiley, p. 255–292.

Boerrigter, S. X. M., Josten, G. P. H., van de Streek, J., Hollander, F. F. A., Los, J., Cuppen, H. M., Bennema, P., and Meekes, H., 2004, MONTY: Monte Carlo Crystal Growth on Any Crystal Structure in Any Crystallographic Orientation; Application to Fats: The Journal of Physical Chemistry A, v. 108, n. 27, p. 5894–5902, https://doi.org/10.1021/jp049804h

Bortz, A. B., Kalos, M. H., and Lebowitz, J. L., 1975, A new algorithm for Monte Carlo simulation of Ising spin systems: Journal of Computational Physics, v. 17, n. 1, p. 10–18, https://doi.org/10.1016/0021-9991(75)90060-1

Bracco, J. N., Grantham, M. C., and Stack, A. G., 2012, Calcite Growth Rates As a Function of Aqueous Calcium-to-Carbonate Ratio, Saturation Index, and Inhibitor Concentration: Insight into the Mechanism of Reaction and Poisoning by Strontium: Crystal Growth & Design, v. 12, n. 7, p. 3540–3548, https://doi.org/10.1021/cg300350k

Bracco, J. N., Stack, A. G., and Steefel, C. I., 2013, Upscaling Calcite Growth Rates from the Mesoscale to the Macroscale: Environmental Science & Technology, v. 47, n. 13, p. 7555–7562, https://doi.org/10.1021/es400687r

Brantley, S. L., Kubicki, J. D., and White, A. F., editors, 2008, Kinetics of Water-Rock Interaction: New York, Springer-Verlag, https://doi.org/10.1007/978-0-387-73563-4

Briese, L., Arvidson, R. S., and Luttge, A., 2017, The effect of crystal size variation on the rate of dissolution – A kinetic Monte Carlo study: Geochimica et Cosmochimica Acta, v. 212, p. 167–175, https://doi.org/10.1016/j.gca.2017.06.010

Burton, W. K., Cabrera, N., and Frank, F. C., 1951, The growth of crystals and the equilibrium structure of their surfaces: Philosophical Transactions of the Royal Society of London, Series A, Mathematical, Physical Science and Engineering Sciences, v. 243, p. 299–358, https://doi.org/10.1098/rsta.1951.0006

Cama, J., Zhang, L., Soler, J. M., Giudici, G. D., Arvidson, R. S., and Lüttge, A., 2010, Fluorite dissolution at acidic pH: *In situ* AFM and *ex situ* VSI experiments and Monte Carlo simulations: Geochimica et Cosmochimica Acta, v. 74, n. 15, p. 4298–4311, https://doi.org/10.1016/j.gca.2010.04.067

Campbell, C. T., Árnadóttir, L., and Sellers, J. R. V., 2013, Kinetic Prefactors of Reactions on Solid Surfaces: Zeitschrift für Physikalische Chemie, v. 227, n. 9–11, p. 1435–1454, https://doi.org/10.1524/zpch.2013.0395

Casey, W. H., and Swaddle, T. W., 2003, Why small? The use of small inorganic clusters to understand mineral surface and dissolution reactions in geochemistry: Reviews of Geophysics, v. 41, n. 2, p. 1008, https://doi.org/10.1029/2002RG000118

Chen, J.-C., Reischl, B., Spijker, P., Holmberg, N., Laasonen, K., and Foster, A. S., 2014, *Ab initio* Kinetic Monte Carlo simulations of dissolution at the NaCl–water interface: Physical Chemistry Chemical Physics, v. 16, n. 41, p. 22545–22554, https://doi.org/10.1039/C4CP02375G

Cheng, V. K. W., and Coller, B. A. W., 1987, Monte Carlo simulation study on the dissolution of a train of infinitely straight steps and of an infinitely straight crystal edge: Journal of Crystal Growth, v. 84, n. 3, p. 436–454, https://doi.org/10.1016/0022-0248(87)90274-0

Cheng, V. K. W., Tang, E. C. M., and Tang, T. B., 1989, The kinetic asymmetry between nucleation growth and dissolution: A Monte Carlo study: Journal of Crystal Growth, v. 96, n. 2, p. 293–303, https://doi.org/10.1016/0022-0248(89)90526-5

Cherepanova, T. A., 1981, Kinetic equation theory and Monte Carlo computer simulation of multicompo-

nent crystal growth: Journal of Crystal Growth, v. 52, Part 1, p. 319–326, https://doi.org/10.1016/0022-0248(81)90211-6

Chernov, A. A., 1961, The Spiral Growth of Crystals: Soviet Physics Uspekhi, v. 4, n. 1. p. 116, https://doi.org/10.1070/PU1961v004n01ABEH003328

Chou, L., Garrels, R. M., and Wollast, R., 1989, Comparative study of the kinetics and mechanisms of dissolution of carbonate minerals: Chemical Geology, v. 78, n. 3–4, p. 269–282, https://doi.org/10.1016/0009-2541(89)90063-6

Churakov, S. V., Labbez, C., Pegado, L., and Sulpizi, M., 2014, Intrinsic Acidity of Surface Sites in Calcium Silicate Hydrates and Its Implication to Their Electrokinetic Properties: The Journal of Physical Chemistry C, v. 118, n. 22, p. 11752–11762, https://doi.org/10.1021/jp502514a

Colombani, J., 2016, The Alkaline Dissolution Rate of Calcite: The Journal of Physical Chemistry Letters, v. 7, n. 13, p. 2376–2380, https://doi.org/10.1021/acs.jpclett.6b01055

Cygan, R. T., Liang, J.-J., and Kalinichev, A. G., 2004, Molecular Models of Hydroxide, Oxyhydroxide, and Clay Phases and the Development of a General Force Field: The Journal of Physical Chemistry B, v. 108, n. 4, p. 1255–1266, https://doi.org/10.1021/jp0363287

Daval, D., Hellmann, R., Saldi, G. D., Wirth, R., and Knauss, K. G., 2013, Linking nm-scale measurements of the anisotropy of silicate surface reactivity to macroscopic dissolution rate laws: New insights based on diopside: Geochimica et Cosmochimica Acta, v. 107, p. 121–134, https://doi.org/10.1016/j.gca.2012.12.045

de Leeuw, N. H., and Parker, S. C., 1998, Surface Structure and Morphology of Calcium Carbonate Polymorphs Calcite, Aragonite, and Vaterite: An Atomistic Approach: The Journal of Physical Chemistry B, v. 102, n. 16, p. 2914–2922, https://doi.org/10.1021/jp973210f

de Leeuw, N. H., Parker, S. C., and Harding, J. H., 1999, Molecular dynamics simulation of crystal dissolution from calcite steps: Physical Review B, v. 60, p. 13792–13799, https://doi.org/10.1103/PhysRevB.60.13792

De Yoreo, J. J., and Vekilov, P. G., 2003, Principles of Crystal Nucleation and Growth: Reviews in Mineralogy and Geochemistry, v. 54, n. 1, p. 57–93, https://doi.org/10.2113/0540057

De Yoreo, J. J., Zepeda-Ruiz, L. A., Friddle, R. W., Qiu, S. R., Wasylenki, L. E., Chernov, A. A., Gilmer, G. H., and Dove, P. M., 2009, Rethinking Classical Crystal Growth Models through Molecular Scale Insights: Consequences of Kink-Limited Kinetics: Crystal Growth & Design, v. 9, n. 12, p. 5135–5144, https://doi.org/10.1021/cg900543g

Dennington, R., Keith, T. A., and Millam, J. M., 2009, GaussView, Version 5: Shawnee, Kansas, Semichem Inc.

Dirichlet, G. L., 1850, Über die Reduction der positiven quadratischen Formen mit drei unbestimmten ganzen Zahlen.: Journal für die reine und angewandte Mathematik, v. 1850, n. 40, p. 209–227, https://doi.org/10.1515/crll.1850.40.209

Dove, P. M., Han, N., and De Yoreo, J. J., 2005, Mechanisms of classical crystal growth theory explain quartz and silicate dissolution behavior: Proceedings of the National Academy of Sciences of the United States of America, v. 102, n. 43, p. 15357–15362, https://doi.org/10.1073/pnas.0507777102

Duckworth, O. W., and Martin, S. T., 2004, Dissolution rates and pit morphologies of rhombohedral carbonate minerals: American Mineralogist, v. 89, n. 4, p. 554–563, https://doi.org/10.2138/am-2004-0410

Emmanuel, S., 2015, Short Communication: Evidence for non-Gaussian distribution of rock weathering rates: Earth Surface Dynamics, v. 3, p. 441–445, https://doi.org/10.5194/esurf-3-441-2015

Evans, M. G., and Polanyi, M., 1935, Some applications of the transition state method to the calculation of reaction velocities, especially in solution: Transactions of the Faraday Society, v. 31, p. 875–894. https://doi.org/10.1039/TF9353100875

Exner, K. S., Heß, F., Over, H., and Seitsonen, A. P., 2015, Combined experiment and theory approach in surface chemistry: Stairway to heaven?: Surface Science, v. 640, p. 165–180, https://doi.org/10.1016/j.susc.2015.01.006

Eyring, H., 1935, The Activated Complex in Chemical Reactions: The Journal of Chemical Physics, v. 3, n. 2, p. 107–115, https://doi.org/10.1063/1.1749604

Fischer, C., Arvidson, R. S., and Lüttge, A., 2012, How predictable are dissolution rates of crystalline material?: Geochimica et Cosmochimica Acta, v. 98, p. 177–185, https://doi.org/10.1016/j.gca.2012.09.011

Fischer, C., Kurganskaya, I., Schäfer, T., and Lüttge, A., 2014, Variability of crystal surface reactivity: What do we know?: Applied Geochemistry, v. 43, p. 132–157, https://doi.org/10.1016/j.apgeochem.2014.02.002

Fischer, C., Kurganskaya, I., and Luttge, A., 2018, Inherited control of crystal surface reactivity: Applied Geochemistry, v. 91, p. 140–148, https://doi.org/10.1016/j.apgeochem.2018.02.003

Frenkel, D., and Smith, B., 2002, Understanding Molecular Simulation: Academic Press, Computational Science Series, v. 1, 664 p., https://doi.org/10.1016/B978-0-12-267351-1.X5000-7

Gaigeot, M.-P., and Sulpizi, M., 2016, Mineral–Water Interaction, *in* Kubicki, J. D., editor, Molecular Modeling of Geochemical Reactions: Chichester, United Kingdom, John Wiley & Sons, Ltd, p. 271–309, https://doi.org/10.1002/9781118845226.ch8

Gale, J. D., Raiteri, P., and van Duin, A. C. T., 2011, A reactive force field for aqueous-calcium carbonate systems: Physical Chemistry Chemical Physics, v. 13, n. 37, p. 16666–16679, https://doi.org/10.1039/c1cp21034c

Gillespie, D. T., 1976, A general method for numerically simulating the stochastic time evolution of coupled chemical reactions: Journal of Computational Physics, v. 22, n. 4, p. 403–434, https://doi.org/10.1016/0021-9991(76)90041-3

Gilmer, G. H., 1976, Growth on imperfect crystal faces: I. Monte-Carlo growth rates: Journal of Crystal Growth, v. 36, n. 1, p. 15–28, https://doi.org/10.1016/0022-0248(76)90209-8

Giudici, G. D., 2002, Surface control vs. diffusion control during calcite dissolution: Dependence of

step-edge velocity upon solution pH: American Mineralogist, v. 87, n. 10, p. 1279–1285, https://doi.org/10.2138/am-2002-1002

Gratz, A. J., and Bird, P., 1993a, Quartz dissolution: Negative crystal experiments and a rate law: Geochimica et Cosmochimica Acta, v. 57, n. 5, p. 965–976, https://doi.org/10.1016/0016-7037(93)90033-S

—— 1993b, Quartz dissolution: Theory of rough and smooth surfaces: Geochimica et Cosmochimica Acta, v. 57, n. 5, p. 977–989, https://doi.org/10.1016/0016-7037(93)90034-T

Gratz, A. J., Manne, S., and Hansma, P. K., 1991, Atomic Force Microscopy of Atomic-Scale Ledges and Etch Pits Formed During Dissolution of Quartz: Science, v. 251, n. 4999, p. 1343–1346, https://doi.org/10.1126/science.251.4999.1343

Grimbergen, R. F. P., Meekes, H., Bennema, P., Strom, C. S., and Vogels, L. J. P., 1998, On the prediction of crystal morphology. I. The Hartman–Perdok Theory Revisited: Acta Crystallographica Section A, v. 54, p. 491–500, https://doi.org/10.1107/S0108767397019806

Grimbergen, R. F. P., Bennema, P., and Meekes, H., 1999, On the prediction of crystal morphology. III. Equilibrium and growth behaviour of crystal faces containing multiple connected nets. Acta Crystallographica Section A, v. 55, p. 84–94, https://doi.org/10.1107/S0108767398008897

Gross, A., 2000, *Ab initio* Molecular Dynamics Simulations of Reactions at Surfaces: Physica Status Solidi (B), v. 217, n. 1, p. 389–404, https://doi.org/10.1002/(SICI)1521-3951(200001)217:1<389::AID-PSSB389>3.0.CO;2-%23

Hess, F., and Over, H., 2017, Rate-Determining Step or Rate-Determining Configuration? The Deacon Reaction over RuO_2(110) Studied by DFT-Based KMC Simulations: ACS Catalysis, v. 7, n. 1, p. 128–138, https://doi.org/10.1021/acscatal.6b02575

Hillner, P. E., Manne, S., Gratz, A. J., and Hansma, P. K., 1992, AFM images of dissolution and growth on a calcite crystal: Ultramicroscopy, v. 42–44, Part 2, p. 1387–1393, https://doi.org/10.1016/0304-3991(92)90454-R

Høgberget, J., Røyne, A., Dysthe, D. K., and Jettestuen, E., 2016, Microscopic modeling of confined crystal growth and dissolution: Physical Review E, v. 94, n. 2, p. 023005, https://doi.org/10.1103/PhysRevE.94.023005

Honess, A. P., 1927, The nature, origin and interpretation of the etch figures on crystals: New York, Wiley, 171 p.

Hull, D., and Bacon, D. J., 2011, Chapter 4 - Elastic Properties of Dislocations, *in* Hull, D. and Bacon, D. J. editors, Introduction to Dislocations (Fifth Edition): Oxford, Butterworth-Heinemann, p. 63–83, https://doi.org/10.1016/B978-0-08-096672-4.00004-9

Humphrey, W., Dalke, A., and Schulten, K., 1996, VMD: Visual molecular dynamics: Journal of Molecular Graphics, v. 14, n. 1, p. 33–38, https://doi.org/10.1016/0263-7855(96)00018-5

Hunter, J. D., 2007, Matplotlib: A 2D Graphics Environment: Computing in Science & Engineering, v. 9, n. 3, p. 90–95, https://doi.org/10.1109/MCSE.2007.55

Jansen, A. P. J., 2012, An Introduction to Kinetic Monte Carlo Simulations of Surface Reactions: Berlin, Heidelberg, Germany, Springer-Verlag, Lecture Notes in Physics, v. 856, 272 p., https://doi.org/10.1007/978-3-642-29488-4

Johnson, J. K., Panagiotopoulos, A. Z., and Gubbins, K. E., 1994, Reactive canonical Monte Carlo: Molecular Physics, v. 81, n. 3, p. 717–733, https://doi.org/10.1080/00268979400100481

Kerisit, S., and Parker, S. C., 2004, Free Energy of Adsorption of Water and Metal Ions on the {1014} Calcite Surface: Journal of the American Chemical Society, v. 126, n. 32, p. 10152–10161, https://doi.org/10.1021/ja0487776

King, H. E., and Putnis, C. V., 2013, Direct observations of the influence of solution composition on magnesite dissolution: Geochimica et Cosmochimica Acta, v. 109, p. 113–126, https://doi.org/10.1016/j.gca.2013.01.032

Klasa, J., Ruiz-Agudo, E., Wang, L. J., Putnis, C. V., Valsami-Jones, E., Menneken, M., and Putnis, A., 2013, An atomic force microscopy study of the dissolution of calcite in the presence of phosphate ions: Geochimica et Cosmochimica Acta, v. 117, p. 115–128, https://doi.org/10.1016/j.gca.2013.03.025

Klyukin, K., Rosso, K. M., and Alexandrov, V., 2018, Iron Dissolution from Goethite (α-FeOOH) Surfaces in Water by *Ab Initio* Enhanced Free-Energy Simulations: The Journal of Physical Chemistry C, v. 122, n. 28, p. 16086–16091, https://doi.org/10.1021/acs.jpcc.8b03743

Kohler, F., Gagliardi, L., Pierre-Louis, O., and Dysthe, D. K., 2018, Cavity Formation in Confined Growing Crystals: Physical Review Letters, v. 121, n. 9, p. 096101, https://doi.org/10.1103/PhysRevLett.121.096101

Kossel, W., 1927, Extending the Law of Bravais: Nachrichten von der Gesellschaft der Wissenschaften zu Göttingen, 143 p.

Kubicki, J. D., 2016, Molecular Modeling of Geochemical Reactions: An Introduction: New York, Wiley, 422 p.

Kubicki, J. D., Sofo, J. O., Skelton, A. A., and Bandura, A. V., 2012, A New Hypothesis for the Dissolution Mechanism of Silicates: The Journal of Physical Chemistry C, v. 116, n. 33, p. 17479–17491, https://doi.org/10.1021/jp300623v

Kühne, T. D., 2014, *Ab-Initio* Molecular Dynamics: Wiley Interdisciplinary Reviews: Computational Molecular Science, v. 4, n. 4, p. 391–406, https://doi.org/10.1002/wcms.1176

Kurganskaya, I., and Churakov, S. V., 2018, Carbonate Dissolution Mechanisms in the Presence of Electrolytes Revealed by Grand Canonical and Kinetic Monte Carlo Modeling: The Journal of Physical Chemistry C, v. 122, n. 51, p. 29285–29297, https://doi.org/10.1021/acs.jpcc.8b08986

Kurganskaya, I., and Luttge, A., 2013a, A comprehensive stochastic model of phyllosilicate dissolution: Structure and kinematics of etch pits formed on muscovite basal face: Geochimica et Cosmochimica Acta, v. 120, p. 545–560, https://doi.org/10.1016/j.gca.2013.06.038

Kurganskaya, I., and Luttge, A., 2013b, Kinetic Monte Carlo Simulations of Silicate Dissolution: Model

Complexity and Parametrization: The Journal of Physical Chemistry C, v. 117, n. 47, p. 24894–24906, https://doi.org/10.1021/jp408845m

—— 2016, Kinetic Monte Carlo Approach To Study Carbonate Dissolution: The Journal of Physical Chemistry C, v. 120, n. 12, p. 6482–6492, https://doi.org/10.1021/acs.jpcc.5b10995

Kurganskaya, I., Arvidson, R. S., Fischer, C., and Luttge, A., 2012, Does the stepwave model predict mica dissolution kinetics?: Geochimica et Cosmochimica Acta, v. 97, p. 120–130, https://doi.org/10.1016/j.gca.2012.08.033

Labbez, C., and Jönsson, B., 2006, A New Monte Carlo Method for the Titration of Molecules and Minerals, *in* International Workshop on Applied Parallel Computing – Applied Parallel Computing. State of the Art in Scientific Computing: Springer, Berlin, Heidelberg, Lecture Notes in Computer Science, v. 4699, p. 66–72, https://doi.org/10.1007/978-3-540-75755-9_8

Labbez, C., Jönsson, B., Pochard, I., Nonat, A., and Cabane, B., 2006, Surface Charge Density and Electrokinetic Potential of Highly Charged Minerals: Experiments and Monte Carlo Simulations on Calcium Silicate Hydrate: The Journal of Physical Chemistry B, v. 110, n. 18, p. 9219–9230, https://doi.org/jp057096+

Laidler, K. J., and King, M. C., 1983, Development of transition-state theory: Journal of Physical Chemistry, v. 87, n. 15, p. 2657–2664, https://doi.org/10.1021/j100238a002

Laio, A., and Parrinello, M., 2002, Escaping free-energy minima: Proceedings of the National Academy of Sciences of the United States of America, v. 99, n. 20, p. 12562–12566, https://doi.org/10.1073/pnas.202427399

Lasaga, A. C., 1995, Fundamental approaches in describing mineral dissolution and precipitation rates: Reviews in Mineralogy and Geochemistry, v. 31, p. 23–8, https://doi.org/10.1515/9781501509650-004

Lasaga, A. C., and Blum, A. E., 1986, Surface chemistry, etch pits and mineral-water reactions: Geochimica et Cosmochimica Acta, v. 50, n. 10, p. 2363–2379, https://doi.org/10.1016/0016-7037(86)90088-8

Lasaga, A. C., and Luttge, A., 2001, Variation of Crystal Dissolution Rate Based on a Dissolution Stepwave Model: Science, v. 291, n. 5512, p. 2400–2404, https://doi.org/10.1126/science.1058173

Lesar, R., 2013, Introduction to Computational Materials Science: Cambridge, United Kingdom, Cambridge University Press, 414 p.

Li, J., Tilbury, C. J., Joswiak, M. N., Peters, B., and Doherty, M. F., 2016, Rate Expressions for Kink Attachment and Detachment During Crystal Growth: Crystal Growth & Design, v. 16, n. 6, p. 3313–3322, https://doi.org/10.1021/acs.cgd.6b00292

Liang, Y., Baer, D. R., McCoy, J. M., Amonette, J. E., and Lafemina, J. P., 1996, Dissolution kinetics at the calcite-water interface: Geochimica et Cosmochimica Acta, v. 60, p. 4883–4887, https://doi.org/10.1016/S0016-7037(96)00337-7

Liu, L.-M., Laio, A., and Michaelides, A., 2011, Initial stages of salt crystal dissolution determined with *ab initio* molecular dynamics: Physical Chemistry Chemical Physics, v. 13, n. 29, p. 13162–13166, https://doi.org/10.1039/c1cp21077g

Luttge, A., and Arvidson, R. S., 2010, Reactions at Surfaces: A New Approach Integrating Interferometry and Kinetic Simulations: Journal of the American Ceramic Society, v. 93, n. 11, p. 3519–3530, https://doi.org/10.1111/j.1551-2916.2010.04141.x

Lüttge, A., Arvidson, R. S., and Fischer, C., 2013, A Stochastic Treatment of Crystal Dissolution Kinetics: Elements, v. 9, n. 3, p. 183–188, https://doi.org/10.2113/gselements.9.3.183

Meakin, P., and Rosso, K. M., 2008, Simple kinetic Monte Carlo models for dissolution pitting induced by crystal defects: The Journal of Chemical Physics, v. 129, p. 204106, https://doi.org/10.1063/1.3021478

Meekes, H., Bennema, P., and Grimbergen, R. F. P., 1998, On the prediction of crystal morphology. II. Symmetry roughening of pairs of connected nets: Acta Crystallographica Section A, v. 54, p. 501–510, https://doi.org/10.1107/S0108767397020357

Michaelis, M., Fischer, C., Colombi Ciacchi, L., and Luttge, A., 2017, Variability of Zinc Oxide Dissolution Rates: Environmental Science & Technology, v. 51, n. 8, p. 4297–4305, https://doi.org/10.1021/acs.est.6b05732

Morrow, C. P., Nangia, S., and Garrison, B. J., 2009, *Ab Initio* Investigation of Dissolution Mechanisms in Aluminosilicate Minerals: The Journal of Physical Chemistry A, v. 113, n. 7, p. 1343–1352, https://doi.org/10.1021/jp8079099

Motzer, C., and Reichling, M., 2010, Morphological classification and quantitative analysis of etch pits: Journal of Applied Physics, v. 108, p. 113523, https://doi.org/10.1063/1.3510535

Murashov, V. V., 2005, Reconstruction of Pristine and Hydrolyzed Quartz Surfaces: The Journal of Physical Chemistry B, v. 109, n. 9, p. 4144–4151, https://doi.org/10.1021/jp0402075

Nangia, S., and Garrison, B. J., 2009, Advanced Monte Carlo Approach To Study Evolution of Quartz Surface during the Dissolution Process: Journal of the American Chemical Society, v. 131, n. 27, p. 9538–9546, https://doi.org/10.1021/ja901305y

—— 2010, Role of Intrasurface Hydrogen Bonding on Silica Dissolution: The Journal of Physical Chemistry C, v. 114, n. 5, p. 2267–2272, https://doi.org/10.1021/jp909878b

Nangia, S., Washton, N. M., Mueller, K. T., Kubicki, J. D., and Garrison, B. J., 2007, Study of a Family of 40 Hydroxylated β-Cristobalite Surfaces Using Empirical Potential Energy Functions: The Journal of Physical Chemistry C, v. 111, n. 13, p. 5169–5177, https://doi.org/10.1021/jp0678608

Nielsen, L. C., DePaolo, D. J., and De Yoreo, J. J., 2012, Self-consistent ion-by-ion growth model for kinetic isotopic fractionation during calcite precipitation: Geochimica et Cosmochimica Acta, v. 86, p. 166–181, https://doi.org/10.1016/j.gca.2012.02.009

Noiriel, C., Oursin, M., Saldi, G., and Haberthür, D., 2018, Direct Determination of Dissolution Rates at Crystal Surfaces Using 3D X-ray Microtomography: ACS Earth and Space Chemistry, v. 3. n. 1, p. 100–108, https://doi.org/10.1021/acsearthspacechem.8b00143

Offeddu, F. G., Cama, J., Soler, J. M., and Putnis, C. V., 2014, Direct nanoscale observations of the coupled

dissolution of calcite and dolomite and the precipitation of gypsum: Beilstein Journal of Nanotechnology, v. 5, p. 1245–1253, https://doi.org/10.3762/bjnano.5.138

Pavese, A., Catti, M., Parker, S. C., and Wall, A., 1996, Modelling of the thermal dependence of structural and elastic properties of calcite, CaCO3: Physics and Chemistry of Minerals, v. 23, n. 2, p. 89–93, https://doi.org/10.1007/BF00202303

Pelmenschikov, A., Strandh, H., Pettersson, L. G. M., and Leszczynski, J., 2000, Lattice Resistance to Hydrolysis of Si−O−Si Bonds of Silicate Minerals: *Ab Initio* Calculations of a Single Water Attack onto the (001) and (111) β-Cristobalite Surfaces: The Journal of Physical Chemistry B, v. 104, n. 24, p. 5779–5783, https://doi.org/10.1021/jp994009r

Pelmenschikov, A., Leszczynski, J., and Pettersson, L. G. M., 2001, Mechanism of Dissolution of Neutral Silica Surfaces: Including Effect of Self-Healing: The Journal of Physical Chemistry A, v. 105, n. 41, p. 9528–9532, https://doi.org/10.1021/jp011820g

Piana, S., and Gale, J. D., 2005, Understanding the Barriers to Crystal Growth: Dynamical Simulation of the Dissolution and Growth of Urea from Aqueous Solution: Journal of the American Chemical Society, v. 127, n. 6, p. 1975–1982, https://doi.org/10.1021/ja043395l

——— 2006, Three-dimensional kinetic Monte Carlo simulation of crystal growth from solution: Journal of Crystal Growth, v. 294, n. 1, p. 46–52, https://doi.org/10.1016/j.jcrysgro.2006.05.020

Piana, S., Reyhani, M., and Gale, J. D., 2005, Simulating micrometre-scale crystal growth from solution: Nature, v. 438, p. 70–73, https://doi.org/10.1038/nature04173

Pitt, I. G., Gilbert, R. G., and Ryan, K. R., 1995, The application of transition state theory to gas–surface reactions in Langmuir systems: The Journal of Chemical Physics, v. 102, p. 3461–3473, https://doi.org/10.1063/1.468583

Pollet-Villard, M., Daval, D., Fritz, B., Knauss, K. G., Schäfer, G., and Ackerer, P., 2016, Influence of etch pit development on the surface area and dissolution kinetics of the orthoclase (001) surface: Chemical Geology, v. 447, p. 79–92, https://doi.org/10.1016/j.chemgeo.2016.09.038

Raiteri, P., Gale, J. D., Quigley, D., and Rodger, P. M., 2010, Derivation of an Accurate Force-Field for Simulating the Growth of Calcium Carbonate from Aqueous Solution: A New Model for the Calcite−Water Interface: The Journal of Physical Chemistry C, v. 114, n. 13, p. 5997–6010, https://doi.org/10.1021/jp910977a

Raiteri, P., Demichelis, R., and Gale, J. D., 2015, Thermodynamically Consistent Force Field for Molecular Dynamics Simulations of Alkaline-Earth Carbonates and Their Aqueous Speciation: The Journal of Physical Chemistry C, v. 119, n. 43, p. 24447–24458, https://doi.org/10.1021/acs.jpcc.5b07532

Rappe, A. K., Casewit, C. J., Colwell, K. S., Goddard III, W. A., and Skiff, W. M., 1992, UFF, a full periodic table force field for molecular mechanics and molecular dynamics simulations: Journal of the American Chemical Society, v. 114, n. 25, p. 10024–10035, https://doi.org/10.1021/ja00051a040

Ratner, M. A., and Schatz, G. C., 2000, Introduction to Quantum Mechanics in Chemistry: Upper Saddle River, New Jersey, Pearson Education, 320 p.

Rohlfs, R. D., Fischer, C., Kurganskaya, I., and Luttge, A., 2018, Crystal Dissolution Kinetics Studied by a Combination of Monte Carlo and Voronoi Methods: Minerals, v. 8, n. 4, p. 133, https://doi.org/10.3390/min8040133

Röder, F., Braatz, R. D., and Krewer, U., 2017, Multi-Scale Simulation of Heterogeneous Surface Film Growth Mechanisms in Lithium-Ion Batteries: Journal of The Electrochemical Society, v. 164, n. 11, p. E3335–E3344, https://doi.org/10.1149/2.0241711jes

Rufe, E., and Hochella, M. F., 1999, Quantitative Assessment of Reactive Surface Area of Phlogopite During Acid Dissolution: Science, v. 285, p. 874–876, https://doi.org/10.1126/science.285.5429.874

Ruiz-Agudo, E., Kowacz, M., Putnis, C. V., and Putnis, A., 2010, The role of background electrolytes on the kinetics and mechanism of calcite dissolution: Geochimica et Cosmochimica Acta, v. 74, n. 4, p. 1256–1267, https://doi.org/10.1016/j.gca.2009.11.004

Senftle, T. P., Hong, S., Islam, M. M., Kylasa, S. B., Zheng, Y., Shin, Y. K., Junkermeier, C., Engel-Herbert, R., Janik, M. J., Aktulga, H. M., Verstraelen, T., Grama, A., and van Duin, A. C. T., 2016, The ReaxFF reactive force-field: Development, applications and future directions: npj Computational Materials, v. 2, p. 15011, https://doi.org/10.1038/npjcompumats.2015.11

Shao, H., Ray, J. R., and Jun, Y.-S., 2011, Effects of salinity and the extent of water on supercritical CO_2-induced phlogopite dissolution and secondary mineral formation: Environmental Science & Technology, v. 45, n. 4, p. 1737–1743, https://doi.org/10.1021/es1034975

Shen, Z., Kerisit, S. N., Stack, A. G., and Rosso, K. M., 2018, Free-Energy Landscape of the Dissolution of Gibbsite at High pH: The Journal of Physical Chemistry Letters, v. 9, n. 7, p. 1809–1814, https://doi.org/10.1021/acs.jpclett.8b00484

Shiraki, R., Rock, P. A., and Casey, W. H., 2000, Dissolution Kinetics of Calcite in 0.1 M NaCl Solution at Room Temperature: An Atomic Force Microscopic (AFM) Study: Aquatic Geochemistry, v. 6, n. 1, p. 87–108, https://doi.org/10.1023/A:1009656318574

Stack, A. G., and Grantham, M. C., 2010, Growth Rate of Calcite Steps As a Function of Aqueous Calcium-to-Carbonate Ratio: Independent Attachment and Detachment of Calcium and Carbonate Ions: Crystal Growth & Design, v. 10, n. 3, p. 1409–1413, https://doi.org/10.1021/cg901395z

Stack, A. G., Raiteri, P., and Gale, J. D., 2012, Accurate Rates of the Complex Mechanisms for Growth and Dissolution of Minerals Using a Combination of Rare-Event Theories: Journal of the American Chemical Society, v. 134, p. 11–14, https://doi.org/10.1021/ja204714k

Stranski, I. N., 1928, Zur Theorie des Kristallwachstums: Zeitschrift für Physikalische Chemie, v. 136, p. 259–278, https://doi.org/10.1515/zpch-1928-13620

Sulpizi, M., Gaigeot, M.-P., and Sprik, M., 2012, The Silica–Water Interface: How the Silanols Determine the Surface Acidity and Modulate the Water Properties: Journal of Chemical Theory and Computation, v. 8, n. 3, p. 1037–1047, https://doi.org/10.1021/ct2007154

Tilbury, C. J., Joswiak, M. N., Peters, B., and Doherty, M. F., 2017, Modeling Step Velocities and Edge Surface Structures during Growth of Non-Centrosymmetric Crystals: Crystal Growth & Design, v. 17, n. 4, p. 2066–2080, https://doi.org/10.1021/acs.cgd.7b00058

Tuckerman, M. E., 2002, *Ab initio* molecular dynamics: Basic concepts, current trends and novel applications: Journal of Physics: Condensed Matter, v. 14, n. 50, p. R1297, https://doi.org/10.1088/0953-8984/14/50/202

Uwaha, M., 2016, Introduction to the BCF theory: Progress in Crystal Growth and Characterization of Materials, v. 62, n. 2, p. 58–68, https://doi.org/10.1016/j.pcrysgrow.2016.04.002

Vinson, M. D., Arvidson, R. S., and Luttge, A., 2007, Kinetic inhibition of calcite (1 0 4) dissolution by aqueous manganese (II): Journal of Crystal Growth, v. 307, n. 1, p. 116–125, https://doi.org/10.1016/j.jcrysgro.2007.05.059

Voronoi, G., 1908a, Nouvelles applications des paramètres continus à la théorie des formes quadratiques. Deuxième mémoire. Recherches sur les parallélloèdres primitifs.: Journal für die reine und angewandte Mathematik, v. 1908, n. 134, p. 198–287, https://doi.org/10.1515/crll.1908.134.198

——— 1908b, Nouvelles applications des paramètres continus à la théorie des formes quadratiques. Premier mémoire. Sur quelques propriétés des formes quadratiques positives parfaites.: Journal für die reine und angewandte Mathematik, v. 1908, v. 133, p. 97–178, https://doi.org/10.1515/crll.1908.133.97

Voter, A., 2007, Introduction to the Kinetic Monte Carlo method, in Sickafus, K. E., and Kotomin, E. A., editors, Radiation Effects in Solids: NATO Science, p. 1–23, https://doi.org/10.1007/978-1-4020-5295-8_1

Wehrli, B., 1989, Monte Carlo simulations of surface morphologies during mineral dissolution: Journal of Colloid and Interface Science, v. 132, n. 1, p. 230–242, https://doi.org/10.1016/0021-9797(89)90232-4

Wolthers, M., Nehrke, G., Gustafsson, J. P., and Van Cappellen, P., 2012, Calcite growth kinetics: Modeling the effect of solution stoichiometry: Geochimica et Cosmochimica Acta, v. 77, p. 121–134, https://doi.org/10.1016/j.gca.2011.11.003

Wolthers, M., Tommaso, D. D., Du, Z., and de Leeuw, N. H., 2013, Variations in calcite growth kinetics with surface topography: Molecular dynamics simulations and process-based growth kinetics modelling: CrystEngComm, v. 15, n. 27, p. 5506–5514, https://doi.org/10.1039/c3ce40249e

Xiao, Y., and Lasaga, A. C., 1996, *Ab initio* quantum mechanical studies of the kinetics and mechanisms of quartz dissolution: OH⁻ catalysis: Geochimica et Cosmochimica Acta, v. 60, n. 13, p. 2283–2295, https://doi.org/10.1016/0016-7037(96)00101-9

Yang, J., and Wang, E. G., 2006, Water adsorption on hydroxylated α-quartz (0001) surfaces: From monomer to flat bilayer: Physical Review B, v. 73, p. 035406, https://doi.org/10.1103/PhysRevB.73.035406

Yang, Y., Min, Y., Lococo, J., and Jun, Y.-S., 2014, Effects of Al/Si ordering on feldspar dissolution: Part I. Crystallographic control on the stoichiometry of dissolution reaction: Geochimica et Cosmochimica Acta, v. 126, p. 574–594, https://doi.org/10.1016/j.gca.2013.10.047

Yanina, S. V., Rosso, K. M., and Meakin, P., 2006, Defect distribution and dissolution morphologies on low-index surfaces of α-quartz: Geochimica et Cosmochimica Acta, v. 70, n. 5, p. 1113–1127, https://doi.org/10.1016/j.gca.2005.11.019

Zhang, J., and Nancollas, G. H., 1990, Kink densities along a crystal surface step at low temperatures and under nonequilibrium conditions: Journal of Crystal Growth, v. 106, n. 2–3, p. 181–190, https://doi.org/10.1016/0022-0248(90)90062-P

——— 1998, Kink Density and Rate of Step Movement during Growth and Dissolution of an *AB* Crystal in a Nonstoichiometric Solution: Journal of Colloid and Interface Science, v. 200, n. 1, p. 131–145, https://doi.org/10.1006/jcis.1997.5357

Zhang, L., and Lüttge, A., 2007, Al,Si order in albite and its effect on albite dissolution processes: A Monte Carlo study: American Mineralogist, v. 92, n. 8–9, p. 1316–1324, https://doi.org/10.2138/am.2007.2471

——— 2008, Aluminosilicate Dissolution Kinetics: A General Stochastic Model: The Journal of Physical Chemistry B, v. 112, n. 6, p. 1736–1742, https://doi.org/10.1021/jp073430l

——— 2009a, Theoretical approach to evaluating plagioclase dissolution mechanisms: Geochimica et Cosmochimica Acta, v. 73, n. 10, p. 2832–2849, https://doi.org/10.1016/j.gca.2009.02.021

——— 2009b, Morphological evolution of dissolving feldspar particles with anisotropic surface kinetics and implications for dissolution rate normalization and grain size dependence: A kinetic modeling study: Geochimica et Cosmochimica Acta, v. 73, n. 22, p. 6757–6770, https://doi.org/10.1016/j.gca.2009.08.010